LETTER

doi:10.1038/nature19318

Serotonin engages an anxiety and fear-promoting circuit in the extended amygdala

Catherine A. Marcinkiewcz[1]*, Christopher M. Mazzone[1,2]*, Giuseppe D'Agostino[3], Lindsay R. Halladay[4], J. Andrew Hardaway[1], Jeffrey F. DiBerto[1], Montserrat Navarro[5], Nathan Burnham[5], Claudia Cristiano[3], Cayce E. Dorrier[1], Gregory J. Tipton[1], Charu Ramakrishnan[6], Tamas Kozicz[7,8], Karl Deisseroth[6], Todd E. Thiele[1,5], Zoe A. McElligott[1,9], Andrew Holmes[4], Lora K. Heisler[3] & Thomas L. Kash[1,2,5,10]

Serotonin (also known as 5-hydroxytryptamine (5-HT)) is a neurotransmitter that has an essential role in the regulation of emotion. However, the precise circuits have not yet been defined through which aversive states are orchestrated by 5-HT. Here we show that 5-HT from the dorsal raphe nucleus (5-HT^{DRN}) enhances fear and anxiety and activates a subpopulation of corticotropin-releasing factor (CRF) neurons in the bed nucleus of the stria terminalis (CRF^{BNST}) in mice. Specifically, 5-HT^{DRN} projections to the BNST, via actions at 5-HT$_{2C}$ receptors (5-HT$_{2C}$Rs), engage a CRF^{BNST} inhibitory microcircuit that silences anxiolytic BNST outputs to the ventral tegmental area and lateral hypothalamus. Furthermore, we demonstrate that this CRF^{BNST} inhibitory circuit underlies aversive behaviour following acute exposure to selective serotonin reuptake inhibitors (SSRIs). This early aversive effect is mediated via the corticotrophin-releasing factor type 1 receptor (CRF$_1$R, also known as CRHR1), given that CRF$_1$R antagonism is sufficient to prevent acute SSRI-induced enhancements in aversive learning. These results reveal an essential 5-HT^{DRN}→CRF^{BNST} circuit governing fear and anxiety, and provide a potential mechanistic explanation for the clinical observation of early adverse events to SSRI treatment in some patients with anxiety disorders[1,2].

Give the multiple converging lines of evidence pinpointing 5-HT as a critical neuromodulator of pathological fear learning[3,4], we first interrogated the endogenous recruitment of the 5-HT$^{DRN→BNST}$ circuit by an aversive footshock stimulus in mice. Using Fluoro-Gold to retrogradely label BNST-projecting 5-HT neurons in the dorsal raphe nucleus (DRN), we found that *c-fos*, an immediate-early gene indicative of *in vivo* neuronal activation, was significantly elevated in 5-HT$^{DRN→BNST}$ neurons after footshock (Fig. 1a–f). Using *in vivo* electrophysiology, we then probed the neuronal dynamics of the BNST during fear conditioning and recall, and found evidence for engagement during both conditioning and recall (Extended Data Fig. 1).

To decipher the role of this 5-HT$^{DRN→BNST}$ circuit in aversive behaviour, Channelrhodopsin2 (ChR2)–eYFP was selectively expressed in 5-HT^{DRN} neurons through the delivery of a Cre-inducible viral vector in mice expressing Cre recombinase under the control of a serotonin transporter promoter (*Sert^{Cre}*) (*Sert* is also known as *Slc6a4*) for both *in vivo* and *ex vivo* analysis. We observed eYFP$^+$ (5-HT) cell bodies in the DRN and eYFP$^+$ fibres in both the dorsal and ventral aspects of the BNST (*Sert^{Cre}*::ChR2$^{DRN→BNST}$), confirming a direct projection of 5-HT neurons originating in the DRN to the BNST (Fig. 1g, h)[5]. Optical stimulation of these fibres in BNST slices evoked 5-HT release, as measured by fast-scan cyclic voltammetry (FSCV) (Fig. 1i, j). Furthermore, bath application of the SSRI fluoxetine reliably decreased the rate of 5-HT reuptake, confirming that photostimulation of SERT$^+$ terminals in the BNST originating from the DRN induces 5-HT release (Fig. 1k, l).

We examined whether this 5-HT$^{DRN→BNST}$ circuit is functionally relevant for fear and anxiety-like behaviour. To investigate this, *Sert^{Cre}*::ChR2$^{DRN→BNST}$ mice were implanted with bilateral optical fibres and photostimulated in the BNST (473 nm, 20 Hz) using a standard tone-shock fear conditioning paradigm. Optogenetic stimulation of this pathway was paired with a tone that co-terminated with a scrambled footshock. Cued fear was assessed 24 h after, and contextual fear 48 h after, the initial fear acquisition session (Fig. 1m, n). Although no changes were observed during fear acquisition, both cued and contextual fear recall were significantly heightened in photostimulated *Sert^{Cre}*::ChR2$^{DRN→BNST}$ mice (Fig. 1o–q). We next assessed anxiety-like behaviour using well-characterized assays: the elevated plus maze (EPM) and novelty-suppressed feeding (NSF) tests. Upon stimulation with light, *Sert^{Cre}*::ChR2$^{DRN→BNST}$ mice exhibited enhanced anxiety-like behaviour in both the EPM and NSF tests (Fig. 1r, s and Extended Data Fig. 2a, b). Importantly, photostimulation did not induce hypolocomotion in the EPM or open field tests, nor did it alter home-cage feeding, thus confirming that hypophagia in the NSF assay was due to anxiety and not a reduction in appetitive drive (Extended Data Fig. 2c–e). One potential explanation of these results is that terminal stimulation in the BNST produces antidromic spikes in DRN cell bodies that release 5-HT in other brain regions, which could be also be driving these behaviours. Therefore we probed the mechanism more deeply using converging approaches.

To determine a receptor target through which 5-HT is signalling in the BNST, we then examined the impact of optogenetically evoked 5-HT^{DRN} release on postsynaptic neuronal excitability and found a 3.05 ± 0.59 mV depolarization that was blocked by a 5-HT$_{2C}$R antagonist (Fig. 1t, u). In contrast to previous reports demonstrating co-release of 5-HT and glutamate from DRN projections to the nucleus accumbens[6], we did not observe any time-locked light-evoked EPSCs in the BNST (data not shown). These results indicate that 5-HT$^{DRN→BNST}$ projections have a predominantly excitatory effect that is dependent on 5-HT$_{2C}$R signalling. To examine the role of 5-HT$_{2C}$R containing neurons in anxiety-like behaviour, we took advantage of a *Htr2c^{Cre}* mouse line (Extended Data Fig. 3a, b)[7]. Using 'designer receptors exclusively activated by designer drugs' (DREADDs) that are coupled to the Gαq signalling pathway (hM3Dq-DREADD)[8], we found that activation of G$_q$ signalling in 5-HT$_{2C}$R-expressing neurons in the BNST significantly delayed the onset of feeding in the NSF assay without affecting home cage feeding behaviour (Extended Data Fig. 3c–g), thus phenocopying the effect observed

[1]Bowles Center for Alcohol Studies, University of North Carolina at Chapel Hill, Chapel Hill, North Carolina 27599, USA. [2]Curriculum in Neurobiology, School of Medicine, University of North Carolina at Chapel Hill School of Medicine, Chapel Hill, North Carolina 27599, USA. [3]Rowett Institute of Nutrition and Health, University of Aberdeen, Aberdeen AB25 2ZD, UK. [4]National Institute on Alcohol Abuse and Alcoholism, National Institutes of Health, Rockville, Maryland 20852-9411, USA. [5]Department of Psychology & Neuroscience, College of Arts and Sciences, University of North Carolina at Chapel Hill, Chapel Hill, North Carolina 27599, USA. [6]Department of Bioengineering, Stanford University, Stanford, California 94305, USA. [7]Hayward Genetics Center, Tulane University, New Orleans, Louisiana 70112, USA. [8]Department of Anatomy, Radboud University Nijmegen Medical Center, 6500HB Nijmegen, The Netherlands. [9]Department of Psychiatry, School of Medicine, University of North Carolina at Chapel Hill, Chapel Hill, North Carolina 27599, USA. [10]Department of Pharmacology, School of Medicine, University of North Carolina at Chapel Hill, Chapel Hill, North Carolina 27599, USA.
*These authors contributed equally to this work.

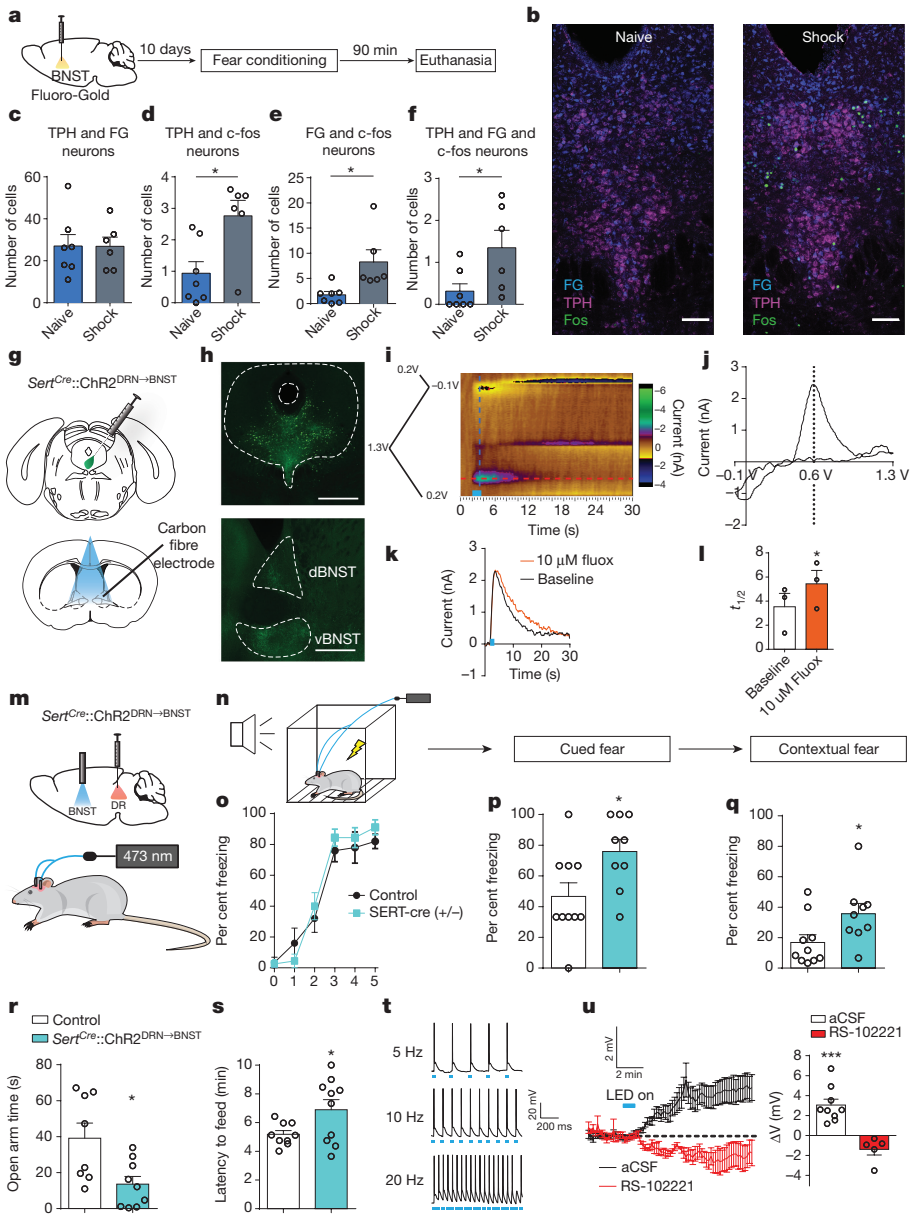

Figure 1 | Optogenetic identification of a 5-HT$^{DRN\rightarrow BNST}$ projection that elicits anxiety and fear-related behaviour. a, Experimental timeline for c-fos labelling of 5-HT$^{DRN\rightarrow BNST}$ neurons following an aversive footshock stimulus. **b**, Representative images of Fluoro-Gold (FG, blue), tryptophan hydroxylase (TPH, violet), and c-fos (green) staining in the DRN for 13 mice. Scale bars, 100 μm. **c–f**, Histograms depicting the number of double- and triple-labelled neurons in the DRN of naive and shocked mice. **c**, There were no significant differences in the number of BNST-projecting 5-HT^{DRN} neurons between groups. **d–f**, Footshock lead to significant elevations in the number of c-fos^{+} 'activated' 5-HT neurons ($t_{11}=2.975$, $P<0.05$, Student's unpaired two-tailed *t*-test, $n=7$ naive and $n=6$ shocked mice), c-fos^{+}, Fluoro-Gold-labelled neurons ($t_{11}=2.836$, $P<0.05$, Student's unpaired two-tailed *t*-test, $n=7$ naive and $n=6$ shocked mice), and triple-labelled neurons ($t_{11}=2.374$, $P<0.05$, Student's unpaired two-tailed *t*-test, $n=7$ naive and $n=6$ shocked mice). **g**, Experimental configuration for light-evoked FSCV experiments in *Sert*^{Cre}::ChR2$^{DRN\rightarrow BNST}$ mice. **h**, Coronal images showing ChR2–YFP expression in the soma of the DRN and axons of the BNST. Scale bars, 500 μm. **i**, Representative colour plot of 5-HT release to optical stimulation (blue bar, 20 Hz, 20 pulses) for 3 mice. **j**, Representative cyclic voltammogram at peak 5-HT (black dashed line) for 3 mice. **k**, Representative current versus time trace at baseline (black) and following 10 μM fluoxetine (red) for 3 mice. **l**, Clearance half-life of 5-HT at baseline (white) and following 10 μM fluoxetine (red). $t_2=8.43$, $P<0.05$, Student's paired two-tailed *t*-test, $n=3$ slices from 3 mice. **m**, *Sert*^{Cre} mice were transduced in the DRN and implanted with bilateral optical fibres in the BNST. **n**, Schematic of fear conditioning procedures in *Sert*^{Cre}::ChR2$^{DRN\rightarrow BNST}$ mice. **o–q**, Photostimulation during fear acquisition had no effect on freezing behaviour during fear learning but increased freezing during cued ($t_{17}=2.436$, $P<0.05$, Student's unpaired two-tailed *t*-test, $n=10$ control, $n=9$ ChR2) and contextual fear recall ($t_{17}=2.271$, $P<0.05$, Student's unpaired two-tailed *t*-test, $n=10$ control, $n=9$ ChR2). **r**, Light delivery to the BNST reduced open arm time in the EPM ($t_{15}=2.79$, $P<0.05$, Student's unpaired two-tailed *t*-test, $n=8$ control, $n=9$ ChR2). **s**, Increased latency to feed in the NSF ($t_{17}=2.19$, $P<0.05$, Student's unpaired two-tailed *t*-test, $n=9$ control, $n=10$ ChR2). **t**, Action potentials generated by photostimulation in the DRN (5 Hz (top), 10 Hz (middle), 20 Hz (bottom), 473 nm). **u**, Depolarization in cells ($t_8=5.20$, $P<0.01$, one-sample *t*-test, $n=9$ cells from 4 mice) after photostimulation in the BNST (5 Hz, 10 s, 473 nm) and blockade of this response by 5 μM RS-102221 (5-HT$_{2C}$R antagonist) ($t_4=2.5$, $P>0.05$, one-sample *t*-test, $n=5$ cells from 2 mice). Data are mean ± s.e.m. *$P<0.05$; ***$P<0.001$.

with 5-HT$^{DRN\rightarrow BNST}$ fibre stimulation during NSF. Together, these results provide converging evidence that activation of 5-HT$^{DRN\rightarrow BNST}$ inputs elicits anxiety-like behaviour via 5-HT$_{2C}$R signalling.

We considered the neurochemical phenotype of these target 5-HT$^{DRN\rightarrow}$5-HT$_{2C}$R^{BNST} neurons and hypothesized that 5-HT via 5-HT$_{2C}$R modulates the activity of neurons expressing the neuropeptide

CRF. This hypothesis was based on a previous analysis of 5-HT_{2C}R knockout mice, which exhibit an anxiolytic phenotype associated with a reduction of c-fos in CRF^{BNST} neurons[9]. Initially, using CRF reporter mice to *a priori* select CRF neurons for recordings, we found a heterogeneous 5-HT-induced response in CRF^{BNST} neurons (Extended Data Fig. 4a), with only a subset demonstrating a depolarization. Consistent with this, double fluorescence *in situ* hybridization revealed that only a subset of CRF neurons within the dorsal BNST (~70%) and ventral BNST (~43%) express 5-HT_{2C}Rs (Extended Data Fig. 4b–d).

Although CRF signalling within the BNST is associated with anxiety-like behaviour[10,11], more recent studies using circuit-based tools have found that optogenetic stimulation of GABAergic projections (which include CRF^{BNST} neurons) to the ventral tegmental area (VTA) are anxiolytic[12]. This led us to hypothesize the existence of functionally distinct subsets of CRF^{BNST} neurons that gate different behaviours and are differentially sensitive to 5-HT. We used fluorescent retrograde tracer beads to label CRF^{BNST} neurons as VTA-projecting or non-VTA-projecting (Fig. 2a), and found that VTA-projecting CRF neurons ($CRF^{BNST\rightarrow VTA}$ neurons) were hyperpolarized by an average of 5.73 ± 1.24 mV and non-VTA-projecting CRF neurons were depolarized by an average of 2.74 ± 0.39 mV during 5-HT bath application. Moreover, the excitatory response to 5-HT in non-VTA-projecting CRF neurons was reversed in the presence of a 5-HT_{2C} receptor antagonist (Fig. 2b). Furthermore, all $CRF^{BNST\rightarrow VTA}$ neurons were non-responsive to the 5-HT_2R agonist meta-chlorophenylpiperazine (mCPP), whereas all non-VTA projecting CRF neurons were depolarized by mCPP by an average of 3.26 ± 0.74 mV (Extended Data Fig. 4e–h). These findings suggest an anatomically distinct response to 5-HT by different subsets of CRF^{BNST} neurons. The subset of CRF^{BNST} neurons expressing 5-HT_{2C}Rs do not project to the VTA and are depolarized by 5-HT, whereas the $CRF^{BNST\rightarrow VTA}$ neurons are hyperpolarized by 5-HT, via actions at another 5-HT receptor.

To determine if this 5-HT-dependent mechanism extended to other anxiolytic efferents, we injected retrograde tracer beads into the lateral hypothalamus (LH) of CRF reporter mice and found 5-HT had similar bidirectional effects on non-LH-projecting and LH-projecting CRF^{BNST} neurons (Extended Data Fig. 5a–c). Noting the functional similarities between these two populations, we used retrograde tracing to determine that roughly ~58% of CRF^{BNST} neurons have projections to the LH or VTA (Extended Data Fig. 5d–f). Notably, ~20–31% of these CRF^{BNST} output neurons form parallel projections to these structures.

In light of recent reports that CRF^{BNST} neurons are exclusively GABAergic[13], we hypothesized that non-VTA-projecting CRF^{BNST} neurons may locally inhibit BNST→VTA neurons to promote fear and anxiety. To test this hypothesis, we injected Crf^{Cre} mice with a Cre-inducible ChR2 into the BNST and retrograde tracer beads into the VTA. We then recorded light-evoked inhibitory postsynaptic potentials (IPSCs) from non-ChR2 (ChR2-negative, retrograde tracer-positive) VTA-projecting BNST neurons (Fig. 2c). Photostimulation produced action potentials in CRF^{BNST} neurons and light-evoked IPSCs in non-ChR2 VTA-projecting neurons, indicating that CRF^{BNST} neurons form local GABAergic synapses with BNST neurons that project to the VTA. Repeating these same experiments in Crf^{Cre}::$ChR2^{BNST}$ mice with retrograde tracer beads in the LH, we found that we could evoke GABA currents using photostimulation in LH-projecting neurons as well (Extended Data Fig. 5g–i). Moreover, we observed that 5-HT increased GABAergic transmission on to BNST→VTA projecting neurons in a tetrodotoxin and 5-HT_{2C}R antagonist dependent manner (Fig. 2d–f and Extended

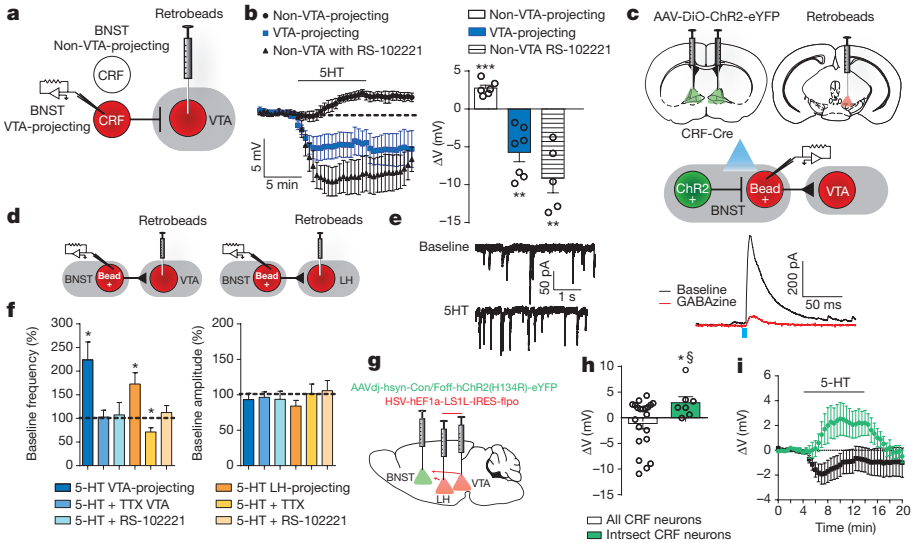

Figure 2 | Serotonin activates a local population of CRF^{BNST} neurons that inhibits outputs to the midbrain. a, Recording scheme for CRF reporter mice injected with retrograde tracer beads in the VTA. **b**, 5-HT depolarizes local CRF neurons ($t_5 = 7.06$, $P < 0.001$, one-sample *t*-test, $n = 6$ cells from 4 mice) in the BNST while hyperpolarizing $CRF^{BNST\rightarrow VTA}$ neurons ($t_6 = 4.64$, $P < 0.01$, one-sample *t*-test, $n = 7$ cells from 6 mice). Non-VTA-projecting CRF neurons are hyperpolarized by 5-HT in the presence of the 5-HT_{2C}R antagonist RS-102221 ($t_4 = 4.74$, $P < 0.01$, one-sample *t*-test, $n = 5$ cells from 3 mice). **c**, Top and middle, schematic depicting infusions and recording configuration for Crf^{Cre}:$ChR2^{BNST}$ mice injected with retrograde tracer beads in the VTA. Bottom, representative trace of light-evoked IPSC in beaded (that is, VTA projecting), non-ChR2 expressing neurons in the BNST of Crf^{Cre}:ChR2 mice with retrograde tracer beads in the VTA ($n = 8$ cells from 3 mice) and blockade of this response by GABAzine ($F_{11,33} = 53.16$, $P < 0.001$, repeated measures one-way ANOVA, $n = 4$ cells from 3 mice). **d**, Recording scheme for C57BL/6 mice with retrograde tracer beads in the VTA or LH. **e**, Representative traces of sIPSCs in BNST neurons that project to the VTA before and after 5-HT application for 5 cells from 4 mice. **f**, Bar graphs showing magnitude of 5-HT effect on average sIPSC frequency in BNST neurons that project to the VTA ($t_4 = 3.257$, $P < 0.05$, one-sample *t*-test, $n = 5$ cells from 4 mice) and in BNST neurons that project to the LH ($t_5 = 3.027$, $P < 0.05$, one-sample *t*-test, $n = 6$ cells from 3 mice) and blockade of these responses by tetrodotoxin (TTX) and RS-102221. Effects on amplitude were non-significant. **g**, Experimental scheme for experiments with Crf^{Cre}::Intrsect–$ChR2^{BNST}$mice. **h**, **i**, 5-HT significantly depolarizes non-projecting CRF (Intrsect) neurons in the BNST ($t_6 = 2.501$, $P < 0.05$, one-sample *t*-test, $n = 7$ cells from 5 mice) and produces a significant change in membrane potential in CRF Intrsect neurons compared to all CRF neurons ($t_{26} = 2.08$, $P < 0.05$, Student's unpaired two-tailed *t*-test, $n = 21$ cells from 14 mice for experiments in all CRF neurons and $n = 7$ cells from 5 mice for Crf^{Cre}::Intrsect–$ChR2^{BNST}$ experiments). Data are mean ± s.e.m. $^*P < 0.05$; $^{**}P < 0.01$; $^{***}P < 0.001$. § denotes $P < 0.05$ for the Student's unpaired two-tailed *t*-test between all CRF neurons and CRF Intrsect neurons in **h**.

Data Fig. 5j–n). Similar effects of 5-HT on GABAergic transmission were found in BNST→LH projecting neurons (Extended Data Fig. 5o–v). Furthermore, slice recordings in a CRF reporter line indicates that 5-HT does not increase GABAergic transmission on to the general population of CRF^{BNST} neurons nor does it directly excite non-CRF VTA projecting neurons (Extended Data Fig. 6). The 5-HT$_2$R agonist mCPP also increased GABAergic but not glutamatergic transmission in the BNST (Extended Data Fig. 7). Finally, to test if optically evoked 5-HT can inhibit BNST outputs to the VTA, we performed slice recordings in the BNST of *Sert*^{Cre}::ChR2$^{DRN→BNST}$ mice and found that brief photostimulation of 5-HT terminals in the BNST increased spontaneous IPSCs (sIPSCs) on to VTA projecting BNST neurons in a manner similar to bath-applied 5-HT (Extended Data Fig. 8a–c). Together, these experiments indicate that CRF^{BNST} neurons inhibit at least two major BNST outputs to the VTA and LH that are reported to be anxiolytic[12,14], providing mechanistic insight into the aversive actions of 5-HT signalling in the BNST.

We took advantage of a new combinatorial strategy called INTronic Recombinase Sites Enabling Combinatorial Targeting or INTRSECT[15] that allows for direct visualization of these non-projecting, putatively local CRF^{BNST} neurons in the BNST. By coupling retrograde Cre-dependent flippases (HSV-LSL1-mCherry-IRES-flpo) in the VTA and LH with a (Cre_{on}/flp_{off})-Chr2-eYFP viral construct in the BNST of *Crf*^{Cre} mice (*Crf*^{Cre}::Intrsect-ChR2^{BNST} mice), we were able to genetically isolate non-VTA/LH-projecting CRF neurons in the BNST. We also infused a Cre-dependent HSV-mCherry vector in a subset of *Crf*^{Cre}::Intrsect-ChR2^{BNST} mice as a control. In HSV-flpo infused *Crf*^{Cre}::Intrsect-ChR2^{BNST} mice, we observed a significant reduction in YFP^{+} cells in the ventral BNST (Extended Data Fig. 8d–f), indicating that a large proportion of VTA-projecting and LH-projecting CRF^{BNST} neurons are located in the ventral BNST. We also found that 5-HT robustly depolarized these *Crf*^{Cre}::Intrsect-ChR2^{BNST} neurons compared to CRF neurons in general (Fig. 2g–i). Furthermore, we observed light-evoked IPSCs in the BNST of *Crf*^{Cre}::Intrsect-ChR2^{BNST} mice, confirming local GABA release from these neurons (Extended Data Fig. 8g). These results support the existence of a separate population of local CRF^{BNST} neurons that is excited by 5-HT and increases local GABAergic transmission in the BNST, distinct from a population of CRF^{BNST} neurons that project to and release GABA in the VTA or the LH (Extended Data Fig. 8h–j).

To probe the translational relevance of these BNST microcircuits, we adopted a pharmacological approach using SSRIs. SSRIs represent one of the most widely used classes of drugs for psychiatric disorders. One limitation of SSRIs is that acute administration can lead to negative behavioural states[1,2], a finding that is recapitulated in rodent models[3,16–20]. Importantly, the BNST has been demonstrated to be an anatomical site of action for some of the aversive actions of SSRIs in rodents[4]. This provided the opportunity to test our model that 5-HT

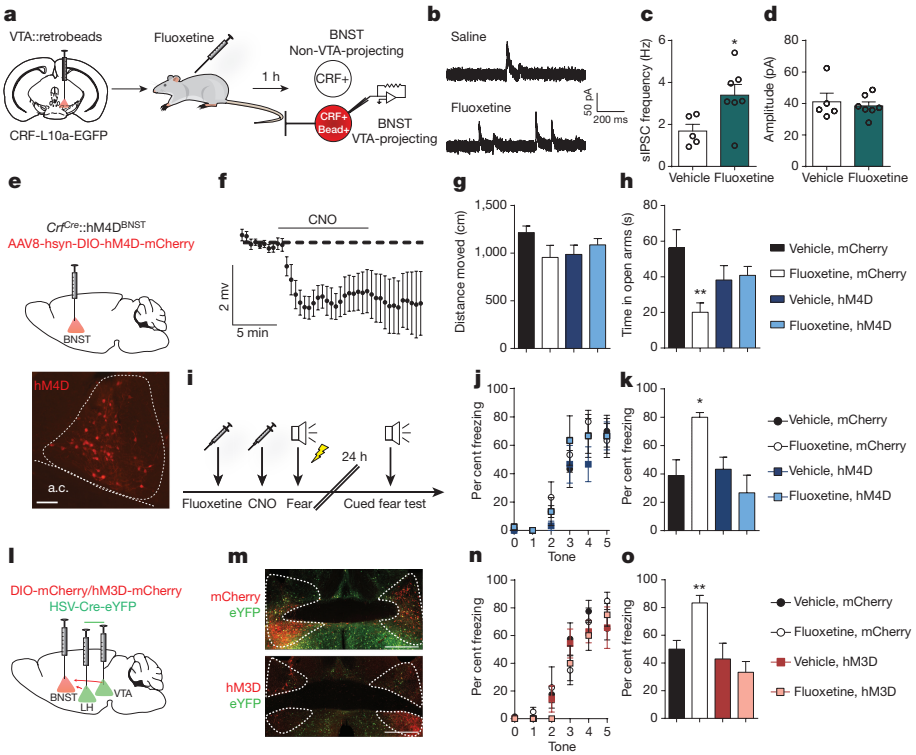

Figure 3 | Acute fluoxetine elicits aversive behaviour by engaging inhibitory CRF circuits in the BNST. a, Schematic of recording for *in vivo* fluoxetine experiments in CRF reporter mice. **b**, Representative traces of sIPSCs in VTA-projecting neurons in the BNST for 5 experiments in 2 saline-treated mice and 7 experiments in 2 fluoxetine-treated mice. **c**, **d**, Bar graphs showing that fluoxetine increases in sIPSC frequency ($t_{10} = 2.55$, $P < 0.05$, Student's unpaired two-tailed *t*-test, $n = 5$ cells from 2 saline-treated mice, $n = 7$ cells from 2 fluoxetine-treated mice), but not amplitude ($t_{10} = 0.4752$, $P > 0.05$, Student's unpaired two-tailed *t*-test, $n = 5$ cells from 2 saline mice, $n = 7$ cells from 2 fluoxetine mice) in VTA-projecting neurons in the BNST. **e**, Experimental configuration for assessment of anxiety in fluoxetine-treated *Crf*^{Cre}:hM4Di^{BNST} (Gi-coupled DREADD) mice and a coronal slice of the BNST expressing hM4Di-mCherry. Scale bar, 100 μm. **f**, Confirmatory electrophysiology in the BNST showing hyperpolarization of hM4Di-mCherry-expressing cells following bath application of CNO ($t_5 = 4.32$, $P < 0.01$, one-sample *t*-test, $n = 6$ cells from 4 mice). **g**, **h**, Chemogenetic silencing of CRF neurons attenuates fluoxetine-induced anxiety like behaviour on the elevated zero maze ($F_{1,30} = 7.086$, $P < 0.05$, two-way ANOVA, $n = 10$ fluoxetine and hM4Di and $n = 8$ for all other groups) without any concomitant locomotor effects. **i**, Experimental configuration for fear conditioning experiments in *Crf*^{Cre}::hM4Di^{BNST} mice. **j**, **k**, Chemogenetic silencing of CRF^{BNST} neurons had no effect on freezing behaviour during fear learning but prevented fluoxetine enhancement of cued fear recall ($F_{1,17} = 8.73$, $P < 0.01$, two-way ANOVA, $n = 6$ mCherry and vehicle and $n = 5$ per group for all other groups). **l**, Experimental configuration for assessment of the role of BNST outputs to the VTA and LH in fluoxetine-induced aversive behaviour. **m**, Confocal image of the BNST from HSV^{Cre}::hM3Dq^{BNST} mice. Scale bars, 500 μm. **n**, **o**, Chemogenetic activation of BNST neurons that project to the midbrain did not impact fear acquisition but attenuated fluoxetine-induced enhancement of cued fear recall ($F_{1,27} = 7.541$, $P < 0.05$, two-way ANOVA, $n = 7$ vehicle/hM3D and $n = 8$ for all other groups). Data are mean ± s.e.m. *$P < 0.05$; **$P < 0.01$.

in the BNST drives aversive behaviour through inhibition of BNST outputs to the VTA. We observed that an acute systemic injection of the SSRI fluoxetine increased GABAergic transmission on to VTA projecting neurons in the BNST (Fig. 3a–d). We then interrogated the role of CRF^{BNST} neurons in acute fluoxetine-enhanced anxiety using Crf^{Cre} mice transduced in the BNST using a Cre-inducible DREADD coupled to the Gαi signalling pathway (hM4Di-DREADD). We found that acute fluoxetine potentiated anxiety-like behaviour, and this effect was blocked by chemogenetic inhibition of CRF^{BNST} neurons (Fig. 3e–h).

To evaluate directly whether endogenous 5-HT acts on CRF^{BNST} neurons to enhance cued fear memory, we used the same chemogenetic approach to silence CRF^{BNST} neurons during fluoxetine treatment and subsequent fear conditioning (Fig. 3i). Chemogenetic inhibition of CRF^{BNST} neurons also significantly attenuated fluoxetine-induced enhancement of cued fear recall, providing proof of concept that augmentation of 5-HT via acute SSRI treatment recruits CRF^{BNST} neurons to enhance fear-related behaviour (Fig. 3j, k). Using connectivity based chemogenetic approaches, we then tested whether inhibition of BNST outputs to the VTA and LH is a critical component of 5-HT→BNST-induced aversive states. We observed that activation of G_q signalling in VTA-projecting and LH-projecting BNST neurons, targeted by HSV-Cre–eYFP infused in the VTA and LH and Cre-dependent Gq-coupled DREADD infused in the BNST (HSV^{Cre}::$hM3Dq^{BNST}$), significantly attenuated fluoxetine enhancement of cued fear recall (Fig. 3l–o). Together, these data provide compelling evidence that acute fluoxetine engenders aversive behaviour by recruiting CRF neurons in the BNST that in turn inhibit putative GABAergic (anxiolytic and stress buffering) outputs from the BNST to the VTA and LH. Pharmacological interventions that target this circuit may improve adverse symptoms during the initial weeks of SSRI treatment. Based on the critical role for CRF^{BNST} neurons in fluoxetine-induced aversive behaviour, we examined the effect of a systemic CRF_1R antagonist on SSRI enhancement of cued fear recall. Blocking the CRF system reduced this aversive state and abolished the increase in sIPSCs in LH-projecting neurons in the BNST during bath application of 5-HT (Extended Data Fig. 9). This provides preclinical evidence that CRF_1R antagonists given in concert with SSRIs could be a promising treatment for anxiety disorders.

Together, these data reveal a discrete 5-HT responsive circuit in the BNST that underlies pathological anxiety and fear associated with a hyperserotonergic state (Extended Data Fig. 10). SSRIs are currently a first-line treatment for anxiety and panic disorders, but can acutely exacerbate symptoms, resulting in poor therapeutic compliance. Our results strongly implicate 5-HT engagement of a local BNST-inhibitory microcircuit in acute SSRI-induced aversive behaviours in rodents, and could potentially be involved in the early adverse events seen in clinical populations, emphasizing the need to identify compounds that selectively target both genetically defined and pathway-specific cell populations.

Online Content Methods, along with any additional Extended Data display items and Source Data, are available in the online version of the paper; references unique to these sections appear only in the online paper.

Received 27 February 2015; accepted 20 July 2016.
Published online 24 August 2016.

1. Gorman, J. M. *et al.* An open trial of fluoxetine in the treatment of panic attacks. *J. Clin. Psychopharmacol.* **7,** 329–332 (1987).
2. Westenberg, H. G. M. & den Boer, J. A. Serotonin-influencing drugs in the treatment of panic disorder. *Psychopathology* **22** (Suppl 1), 68–77 (1989).
3. Burghardt, N. S., Bush, D. E., McEwen, B. S. & LeDoux, J. E. Acute selective serotonin reuptake inhibitors increase conditioned fear expression: blockade with a $5\text{-}HT_{2C}$ receptor antagonist. *Biol. Psychiatry* **62,** 1111–1118 (2007).
4. Ravinder, S., Burghardt, N. S., Brodsky, R., Bauer, E. P. & Chattarji, S. A role for the extended amygdala in the fear-enhancing effects of acute selective serotonin reuptake inhibitor treatment. *Transl. Psychiatry* **3,** e209 (2013).
5. Phelix, C. F., Liposits, Z. & Paull, W. K. Serotonin–CRF interaction in the bed nucleus of the stria terminalis: a light microscopic double-label immunocytochemical analysis. *Brain Res. Bull.* **28,** 943–948 (1992).
6. Liu, Z. *et al.* Dorsal raphe neurons signal reward through 5-HT and glutamate. *Neuron* **81,** 1360–1374 (2014).
7. Burke, L. K. *et al.* Sex difference in physical activity, energy expenditure and obesity driven by a subpopulation of hypothalamic POMC neurons. *Mol. Metab.* **5,** 245–252 (2016).
8. Armbruster, B. N., Li, X., Pausch, M. H., Herlitze, S. & Roth, B. L. Evolving the lock to fit the key to create a family of G protein-coupled receptors potently activated by an inert ligand. *Proc. Natl Acad. Sci. USA* **104,** 5163–5168 (2007).
9. Heisler, L. K., Zhou, L., Bajwa, P., Hsu, J. & Tecott, L. H. Serotonin $5\text{-}HT_{2C}$ receptors regulate anxiety-like behavior. *Genes Brain Behav.* **6,** 491–496 (2007).
10. Olive, M. F., Koenig, H. N., Nannini, M. A. & Hodge, C. W. Elevated extracellular CRF levels in the bed nucleus of the stria terminalis during ethanol withdrawal and reduction by subsequent ethanol intake. *Pharmacol. Biochem. Behav.* **72,** 213–220 (2002).
11. Huang, M. M. *et al.* Corticotropin-releasing factor (CRF) sensitization of ethanol withdrawal-induced anxiety-like behavior is brain site specific and mediated by CRF-1 receptors: relation to stress-induced sensitization. *J. Pharmacol. Exp. Ther.* **332,** 298–307 (2010).
12. Jennings, J. H. *et al.* Distinct extended amygdala circuits for divergent motivational states. *Nature* **496,** 224–228 (2013).
13. Dabrowska, J. *et al.* Neuroanatomical evidence for reciprocal regulation of the corticotrophin-releasing factor and oxytocin systems in the hypothalamus and the bed nucleus of the stria terminalis of the rat: implications for balancing stress and affect. *Psychoneuroendocrinology* **36,** 1312–1326 (2011).
14. Kim, S.-Y. *et al.* Diverging neural pathways assemble a behavioural state from separable features in anxiety. *Nature* **496,** 219–223 (2013).
15. Fenno, L. E. *et al.* Targeting cells with single vectors using multiple-feature Boolean logic. *Nature Methods* **11,** 763–772 (2014).
16. Dekeyne, A., Denorme, B., Monneyron, S. & Millan, M. J. Citalopram reduces social interaction in rats by activation of serotonin $(5\text{-}HT)_{2C}$ receptors. *Neuropharmacology* **39,** 1114–1117 (2000).
17. Belzung, C., Le Guisquet, A. M., Barreau, S. & Calatayud, F. An investigation of the mechanisms responsible for acute fluoxetine-induced anxiogenic-like effects in mice. *Behav. Pharmacol.* **12,** 151–162 (2001).
18. Javelot, H. *et al.* Efficacy of chronic antidepressant treatments in a new model of extreme anxiety in rats. *Depress. Res. Treat.* **2011,** 531435 (2011).
19. Liu, J. *et al.* Acute administration of leptin produces anxiolytic-like effects: a comparison with fluoxetine. *Psychopharmacology* **207,** 535–545 (2010).
20. Mombereau, C., Gur, T. L., Onksen, J. & Blendy, J. A. Differential effects of acute and repeated citalopram in mouse models of anxiety and depression. *Int. J. Neuropsychopharmacol.* **13,** 321–334 (2010).

Acknowledgements We acknowledge B. Roth for providing DREADD viral constructs and $Sert^{Cre}$ mice, and B. Lowell for providing Crf^{Cre} mice. We also thank A. Lopez, D. Perron, and A. Kendra for technical assistance with stereotaxic surgeries on mice, B. Geenen for technical assistance with immunohistochemistry and E. Dankoski for technical assistance with the FSCV. This work was supported by NIH grants AA019454, AA011605 (T.L.K.), the Wellcome Trust (098012) and the Biotechnology and Biological Sciences Research Council grant (BB/K001418/1) (L.K.H.) and by NIH grant K01AA023555 and the Alcohol Beverage Medical Research Fund (Z.A.M.). C.A.M. was supported by a postdoctoral NIAAA F32 fellowship (AA021319-02). C.M.M. is supported by a predoctoral NIAAA F31 fellowship (F31AA023440).

Author Contributions C.A.M., C.M.M., G.D., Z.A.M., L.K.H. and T.L.K. designed the experiments. A.H. and J.F.D. performed triple label fos/tryptophan hydroxylase/Fluor-Gold staining and image analysis. L.R.H. performed electrode placement surgeries and *in vivo* recordings during fear acquisition and recall. C.A.M. performed stereotaxic surgeries for evoked 5-HT electrophysiology and optogenetic behavioural experiments. Z.A.M. performed slice FSCV experiments and C.A.M. performed evoked 5-HT electrophysiology experiments. C.A.M. performed stereotaxic surgeries, behavioural and data analysis for $5\text{-}HT^{DRN\rightarrow BNST}$ optogenetic experiments. C.A.M. performed all slice electrophysiology experiments and C.M.M. and C.A.M. performed stereotaxic surgeries for these experiments (retrograde tracers, ChR2 infusions, and hM3D and hM4D infusions), C.M.M. performed stereotaxic surgeries for chemogenetic manipulations in CRF^{BNST} neurons that were used in fluoxetine fear conditioning experiments and C.A.M. performed behavioural and data analysis. C.E.D. performed surgeries for electrophysiological recordings and data analysis for fear conditioning experiments. M.N. and J.F.D. performed surgeries for chemogenetic manipulations in CRF^{BNST} neurons that were used in fluoxetine anxiety (EZM) assays and N.B. and C.A.M. performed behavioural and data analysis. C.M.M. and J.F.D. performed stereotaxic surgeries for HSV^{Cre}::$hM3D^{BNST}$ behavioural manipulations and C.A.M. performed behavioural and data analysis. C.M.M. also performed imaging and analysis for optogenetic experiments, chemogenetic, and Intrsect experiments. C.R. and K.D. designed Intrsect viral constructs. G.D. and C.C. performed surgeries, behavioural and data analysis for $Htr2c^{Cre}$::$hM3D^{BNST}$ experiments. C.A.M., C.M.M. and T.L.K. wrote the manuscript with input from Z.A.M., L.R.H., J.F.D., J.A.H., G.D., T.E.T., A.H., L.K.H. and T.K.

Author Information Reprints and permissions information is available at www.nature.com/reprints. The authors declare no competing financial interests. Readers are welcome to comment on the online version of the paper. Correspondence and requests for materials should be addressed to T.L.K. (thomas_kash@med.unc.edu).

Reviewer Information *Nature* thanks A. Sahay and the other anonymous reviewer(s) for their contribution to the peer review of this work.

METHODS

Data reporting. Based on power analyses that assumed a normal distribution, a 20% change in mean and 15% variation, we determined that at least 9 mice per group would be needed for behavioral experiments. This was adhered to as far as possible, except in cases where mice had to be removed owing to misplaced injections or lost headcaps. Mice were randomly assigned to groups and attempts were made to balance groups according to variables such as age and housing condition. The investigators were not blinded to allocation during experiments, but were blinded to outcome assessment for all behavioral experiments.

Mice. Mice were used in all experiments. For experiments involving Cre lines, mice were crossed for several generations to C57 mice before using. All wild-type mice were C57BL/6 mice obtained from The Jackson Laboratory (Bar Harbour, ME). For all behavioural experiments except those involving *Htr2c*^{Cre} mice, male mice ranging in age from 8–16 weeks were used. Female *Htr2c*^{Cre} mice were used in chemogenetic manipulations. Both male and female mice aged 6–20 weeks were used for slice electrophysiology and anatomical tracing experiments. All behavioural studies or tissue collection for *ex vivo* slice electrophysiology were performed during the light cycle.

All behavioural experiments in *Htr2c*^{cre} mice were conducted at the University of Aberdeen and in accordance with the United Kingdom Animals (Scientific Procedures) Act of 1986. All *in vivo* electrophysiology experiments were conducted in accordance with all rules and regulations at the National Institute for Alcohol Abuse and Alcoholism at the National Institutes of Health. All other procedures were conducted in accordance with the National Institutes of Health guidelines for animal research and with the approval of the Institutional Animal Care and Use Committee at the University of North Carolina at Chapel Hill.

All animals were group housed on a 12 h light cycle (lights on at 7 a.m.) with *ad libitum* access to rodent chow and water, unless described otherwise. CRF-*ires*-Cre (*Crf*^{cre}) were provided by Bradford Lowell (Harvard University) and were previously described[21]. C57BL/6J mice were obtained from the Jackson Laboratory (Bar Harbour, ME). To visualize CRF-expressing neurons, *Crf*^{Cre} mice were crossed with either an Ai9 or a Cre-inducible L10-GFP reporter line (Jackson Laboratory)[22] to produce CRF-Ai9 or CRF-L10GFP progeny, referred to throughout the manuscript as CRF-reporters. *Sert*^{Cre} mice (from GENSAT) were a generous gift from Bryan Roth. *Htr2c*^{Cre} mice were supplied by Lora Heisler and are described in detail elsewhere[7].

Male mice were used for *in vivo* optogenetic behavioural experiments and for assessing the involvement of BNST CRF neurons on fluoxetine-induced enhancement of fear. Female 5-HT$_{2C}$-Cre mice were used in chemogenetic manipulations. Both male and female mice were used for slice electrophysiology and anatomical tracing experiments. All behavioural studies or tissue collection for *ex vivo* slice electrophysiology were performed during the light cycle.

Viruses and tracers. All AAV viruses except INTRSECT constructs were produced by the Gene Therapy Center Vector Core at the University of North Carolina at Chapel Hill and had titres of $>10^{12}$ genome copies per ml. For *ex vivo* and *in vivo* optical experiments, mice were injected with rAAV5-ef1α-DIO-hChR2(H134R)-eYFP or rAAV5-ef1α-DIO-eYFP as a control. Red IX retrobeads (Lumafluor) were used to fluorescently label LH- and VTA-projecting BNST neurons during *ex vivo* slice electrophysiology recordings. The retrograde tracer Fluoro-Gold (Fluorochrome) was used for anatomical mapping. Choleratoxin B (CTB) 555 and CTB 657 retrograde tracers (Invitrogen; C34776, and C34778, respectively) diluted to 0.5% (w/v) in sterile PBS were used per injection site for anatomical mapping of collateral projections from BNST to LH and VTA. For chemogenetic manipulations, mice were injected with 400 nl of rAAV8-hsyn-DIO-hM3D(Gq)-mCherry, rAAV8-hsyn-DIO-hM4D(Gi)-mCherry, or rAAV8-hsyn-DIO-mCherry bilaterally. HSV-hEF1α-mCherry, HSV-ef1α-LSL1-mCherry-IRES-flpo, and HSV-ef1α-IRES-Cre (supplied by Rachel Neve at the McGovern Institute for Brain Research at MIT) were injected bilaterally into the VTA and LH at a volume of 500 nl per site. The INTRSECT construct AAVdj-hSyn-Con/Foff-hChR2(H134R)-EYFP was infused at 500 nl per side into the BNST. All AAV constructs had viral titres $>10^{12}$ genome particles per ml.

Stereotaxic injections. All surgeries were conducted using aseptic technique. Adult mice (2–5 months) were deeply anaesthetized with 5% isoflurane (v/v) in oxygen and placed into a stereotactic frame (Kopf Instruments) while on a heated pad. Sedation was maintained at 1.5–2.5% isoflurane during surgery. An incision was made down the midline of the scalp and a craniotomy was performed above the target regions and viruses and fluorescent tracers were microinjected using a Neuros Hamilton syringe at a rate of 100 nl min^{-1}. After infusion, the needle was left in place for 10 min to allow for diffusion of the virus before the needle was slowly withdrawn. Injection coordinates (in mm, midline, Bregma, dorsal surface): BNST (±1.00, 0.30, −4.35), LH (±0.9 to 1.10, −1.7, −5.00 to −5.2), VTA (−0.3, −2.9, −4.6), DR (0.0, −4.65, −3.2 with a 23° angle of approach). When using retrobeads, injection volumes into the LH and VTA were 300 nl and 400 nl, respectively. Fluoro-Gold injection volumes were 200 nl per target site. CTB volumes were 200 nl per target site. An optical fibre was implanted in the BNST (±1.00, 0.20, −4.15) at a 10° angle for *in vivo* photostimulation studies. After fibre implantation, dental cement was used to adhere the ferrule to the skull. Following surgery, all mice returned to group housing. Mice were allowed to recover for at least 3 weeks before being used for chemogenetic behavioural studies, or 6 weeks for *in vivo* optogenetic studies.

Drugs. RS-102221, 5-HT and mCPP were from Tocris (Bristol, UK). For electrophysiology experiments, RS-102221 was made up to 100 mM in DMSO and then diluted to a final concentration of 5 μM in aCSF. 5-HT and mCPP were stocked at 10 and 20 mM, respectively, in ddH_2O and diluted to their final concentations in aCSF. For electrophysiology experiments, clozapine-N-oxide (CNO; from Bryan Roth) was stocked at 100 mM in DMSO and diluted to 10 μM in aCSF. For behaviour experiments, CNO was dissolved in 0.5% DMSO (in 0.9% saline) to a concentration of 0.1 mg ml^{-1} or 0.3 mg ml^{-1} and injected at 10 ml per kg for a final concentration of 1 or 3 mg per kg, i.p. Fluoxetine (Sigma) was made up in 0.9% NaCl to a concentration of 1 mg ml^{-1} and then injected at 10 ml per kg for a final concentration of 10 mg per kg, i.p.

***In vivo* electrophysiological procedures.** *Surgical procedures.* Mice were anaesthetized with 2% isoflurane (Baxter Healthcare, Deerfield, IL) and implanted with 2 × 8 electrode (35 μm tungsten) micro-arrays (Innovative Neurophysiology, Durham, NC) targeted at the BNST (ML: 0.8 mm, AP: ± 0.5 mm, and DV: −4.15 mm relative to Bregma). Following surgery, mice were singly housed and allowed at least one week to recover before behavioural testing.

Fear conditioning. Fear conditioning took place in 27 × 27 × 11 cm conditioning chambers (Med Associates, St. Albans, VT), with a metal-rod floor (context A) and scented with 1% vanilla. Mice received 5 parings of a pure tone CS with a 0.6 mA foot shock. 24 h following conditioning, mice underwent a CS recall test (10 presentations of the CS alone, 5 s ITI), which was conducted in a Plexiglas cylinder (20 cm diameter) and scented with 1% acetic acid (context B). Stimulus presentations for both tests were controlled by MedPC (Med Associates, St. Albans, VT). Cameras were mounted overhead for recording freezing behaviour, which was scored automatically using CinePlex Behavioural Research System software (Plexon, Dallas, TX).

Electrophysiological recording and single unit analysis. Electrophysiological recording took place during both fear conditioning and CS recall tests. Individual units were identified and recorded using Omniplex Neural Data Acquisition System (Plexon, Dallas, TX). Neural data was sorted using Offline Sorter (Plexon, Dallas, TX). Waveforms were isolated manually, using principal component analysis. To be included in the analyses, spikes had to exhibit a refractory period of at least 1 ms. Autocorrelograms from simultaneously recorded units were examined to ensure that no cell was counted twice. Single units were analysed by generating perievent histograms (3 s bins) of firing rates from 30 s before CS onset until 30 s after CS offset (NeuroExplorer 5.0, Nex Technologies, Madison, AL). Firing rates were normalized to baseline (30 s before CS onset) using *z*-score transformation. Analysis included a total of 139 cells over three days of recording. Data reported for raw firing rates include only putative principal neurons (<10 Hz).

The formula for computing the suppression ratio was (average freezing rate) / (average freezing rate + average movement rate). Each cell was calculated individually. A value of 0.5 = no change in rate).

Ex vivo *slice electrophysiology.* Brains were sectioned at 0.07 (mm per s) on a Leica 1200S vibratome to obtain 300 μm coronal slices of the BNST, which were incubated in a heated holding chamber containing normal, oxygenated aCSF (in mM:124 NaCl, 4.4 KCl, 2 $CaCl_2$, 1.2 $MgSO_4$, 1 NaH_2PO_4, 10.0 glucose, and 26.0 $NaHCO_3$) maintained at 30 ± 1 °C for at least 1 h before recording. Slices were transferred to a recording chamber (Warner Instruments) submerged in normal, oxygenated aCSF maintained at 28–30 °C at a flow rate of 2 ml min^{-1}. Neurons of the BNST were visualized using infrared differential interference contrast (DIC) video-enhanced microscopy (Olympus). Borosilicate electrodes were pulled with a Flaming-Brown micropipette puller (Sutter Instruments) and had a pipette resistance between 3–6 MΩ. Signals were acquired via a Multiclamp 700B amplifier, digitized at 10 kHz and analysed with Clampfit 10.3 software (Molecular Devices, Sunnyvale, CA, USA).

Light-evoked action potentials. In *Sert*^{Cre} or *Crf*^{Cre} mice, fluorescently labelled neurons expressing ChR2 were visualized and stimulated with a blue (470 nm) LED using a 1 Hz, 2 Hz, 5 Hz, 10 Hz, and 20 Hz stimulation protocol with a pulse width of 0.5 ms. Evoked action potentials were recorded in current clamp mode using a potassium gluconate based internal solution (in mM: 135 K^+ gluconate, 5 NaCl, 2 $MgCl_2$, 10 HEPES, 0.6 EGTA, 4 Na_2ATP, 0.4 Na_2GTP, pH 7.3, 285–290 mOsmol).

Light-evoked synaptic transmission. In *Crf*^{Cre} mice with ChR2 in the BNST and retrograde tracer beads in the VTA or LH, we visualized non-ChR2-expressing, beaded neurons using green (532 nm) LED. Recordings were conducted in voltage

clamp mode using a caesium-methansulfonate (Cs-Meth) based internal solution (in mM: 135 caesium methanesulfonate, 10 KCl, 1 $MgCl_2$, 0.2 EGTA, 2 QX-314, 4 MgATP, 0.3 GTP, 20 phosphocreatine, pH 7.3, 285–290 mOsmol) so that we could detect EPSCs (−55 mV) and IPSCs (+10 mV) in the same neuron. After confirming the absence of a light-evoked EPSC signal, we measured light-evoked IPSCs during a single 5-ms light pulse of 470 nm. In a subset of these experiments, SR95531 (GABAzine, 10 μM) was bath applied for 10 min to block IPSCs.

Drug effects in CRF^{BNST} neurons. *Crf*-reporter mice were injected with retrograde tracer beads into the VTA (ML −0.5, AP −2.9, DV −4.6). We then recorded from beaded (VTA-projecting) and non-beaded (non-projecting) CRF neurons in the BNST. Acute drug effects were determined in current clamp mode in the presence of TTX using a potassium gluconate-based internal solution. After a 5-min stable baseline was established, 5-HT (10 μM) or mCPP (20 μM) was bath applied for 10 min while recording changes in membrane potential. The difference in membrane potential between baseline and drug application at peak effect (delta or Δ MP) was later determined. In a subset of mCPP experiments, slices were incubated with RS-102221 (5 μM) for at least 20 min before experiments began.

Synaptic transmission. Spontaneous inhibitory postsynaptic currents (sIPSCs) were assessed in voltage clamp using a potassium-chloride gluconate-based intracellular solution (in mM: 70 KCl, 65 K^+-gluconate, 5 NaCl, 10 HEPES, 0.5 EGTA, 4 ATP, 0.4 GTP, pH 7.2, 285–290 mOsmol). IPSCs were pharmacologically isolated by adding kynurenic acid (3 mM) to the aCSF to block AMPA and NMDA receptor-dependent postsynaptic currents. The amplitude and frequency of sIPSCs were determined from 2 min recording episodes at −70 mV. The baseline was averaged from the 4 min preceding the application of 5-HT (10 μM) or mCPP (10 μM) for 10 min. In a subset of these experiments, RS-102221 (5 μM) was added to the aCSF and slices were incubated in this drug solution for at least 20 min before experiments began. For miniature IPSCs (mIPSCs), TTX was included in the aCSF to block network activity.

In $Sert^{Cre}$::$ChR2^{BNST}$ mice with retrograde tracer beads in the VTA, sIPSCs were recorded as described above. After achieving a stable baseline, a 10 s, 20 Hz photostimulation was applied.

For assessment of spontaneous excitatory postsynaptic currents (sEPSCs), a caesium gluconate-based intracellular solution was used (in mM: 135 Cs^+-gluconate, 5 NaCl, 10 HEPES, 0.6 EGTA, 4 ATP, 0.4 GTP, pH 7.2, 290–295 mOsmol). $AMPA_R$-mediated EPSCs were pharmacologically isolated by adding 25 μM picrotoxin to the aCSF. sEPSC recordings were acquired in 2 min recording blocks at −70 mV.

Fast-scan cyclic voltammetry (FSCV). Electrodes were fabricated as previously described and cut to 50–100 μm in length[23]. Animal and slice preparation were as described above for electrophysiology and slices were perfused on the rig in ACSF. Using a custom-built potentiostat (University of Washington Seattle), 5-HT recordings were made in the BNST using TarHeel CV written in laboratory view (National Instruments). Briefly a triangular waveform (−0.1 V to 1.3 V with a 10% phase shift at 1,000 V per s, versus Ag/AgCl) was applied to the carbon fibre electrode at a rate of 10 Hz. Slices were optically stimulated with 20 5-ms blue (490 nm) light pulses at a rate of 20 Hz down the submerged 40× objective. 10 cyclic voltammograms were averaged before optical stimulation for background subtraction. Voltammograms were digitally smoothed one time with a fast Fourier transform following data collection and analysed with HDCV (UNC Chapel Hill). Fluoxetine (10 μM) was bath applied following a stable baseline (20 min).

Behavioural assays. For chemogenetic manipulations, mice were transported to a holding cabinet adjacent to the behavioural testing room to habituate for at least 30 min before being pretreated with CNO (3 mg per kg, i.p. for Crf^{Cre} mice and 1 mg per kg, i.p. for Htr_{2C}^{Cre} mice). All behavioural testing began 45 min following CNO treatment, with the exception of fear conditioning training, which occurred 30 min after a CNO injection. When assessing the effect of fluoxetine on fear conditioning, fluoxetine (10 mg per kg, i.p.), or vehicle, was administered 1 h before training (30 min before CNO treatment). For optogenetic manipulations, mice received bilateral stimulation (473 nm, ∼10 mW, 5 ms pulses, 20 Hz) when specified. Unless specified, all equipment was cleaned with a damp cloth between mouse trials. All sessions were video recorded and analysed using EthoVision software (Noldus Information Technologies) except where noted.

Elevated plus maze. Mice were placed in the centre of an elevated plus maze and allowed to explore during a 5 min session. Light levels in the open arms were ∼14 lux. During optogenetic manipulations mice received bilateral stimulation during the entire 5 min session. Mice that left the maze were excluded from analysis ($n = 2$ control, 1 ChR2 from optogenetic experiments).

Open field. Mice were placed into the corner of a white Plexiglas open field arena (25 × 25 × 25 cm) and allowed to freely explore for 30 min. The centre of the open field was defined as the central 25% of the arena. For optogenetic studies the 30 min session was divided into three 10-min epochs consisting of stimulation off, stimulation on, and stimulation off periods.

Novelty-induced suppression of feeding. 48 h before testing, mice were provided with access to a single piece of Froot Loops cereal (Kellogg's) in their home cage. 24 h before testing, home cage chow was removed and mouse body weights were recorded. Water remained available *ad libitum*. Beginning at least one hour before testing, mice transferred to new clean cages so they were singly housed for the test session and body weights were recorded. During the test session mice were placed into an arena (25 × 25 × 25 cm) that contained a single Froot Loop on top of a piece of circular filter paper. Mice were monitored by a live observer and the latency for the mouse to begin eating the pellet was measured, allowing up to 10 min. All mice began eating within this time. Following the initiation of feeding, mice were removed from the arena and placed back into their home cages. Mice were then provided with 10 min of access to a pre-weighed amount of Froot Loops for a post-test feeding session. After this 10 min post-test, the remaining Froot Loops were weighed and mice were returned to *ad libitum* home cage chow. Mice were returned to group housing at the end of this session. For optogenetic experiments, mice received constant 20 Hz optical stimulation during both the latency to feed assay and the 10 min post-test. During optogenetic experiments, one control mouse did not feed during the 10 min NSF session and was excluded from the results.

Home cage feeding. $Sert^{Cre}$ mice were food deprived for 24 h. On the day of the experiment, mice were acclimated to the behaviour room for 1 h. A single pre-weighed food pellet was placed in the home cage and the mice were allowed to eat for 10 min during optogenetic stimulation. At the end of the experimental session, the pellet was removed and weighed and mice were given *ad libitum* access to food.

Htr_{2C}^{Cre} mice were acclimated in metabolic chambers (TSE Systems, Germany) for 2 days before the start of the recordings. After acclimation, mice were food deprived for 24 h. Following fasting, mice received an i.p. injection of CNO 30 min before food presented again. Mice were recorded for 12 h with the following measurements being taken every 30 min: water intake, food intake, ambulatory activity (in x and z axes), and gas exchange (O_2 and CO_2) (using the TSE LabMaster system, Germany). Energy expenditure was calculated according to the manufacturer's guidelines (PhenoMaster Software, TSE Systems).

Fear conditioning. We used a three-day protocol to assess both cued and contextual fear recall. On the first day, mice were placed into a fear conditioning chamber (Med Associates) that contained a grid floor and was cleaned with a scented paper towel (19.5% ethanol, 79.5% H_2O, 1% vanilla). After a 3 min baseline period, mice were exposed to a 30 s tone (3 kHz, 80 dB) that co-terminated with a 2 s scrambled foot shock (0.6 mA). A total of 5 tone-shock pairings were delivered with a random inter-tone interval (ITI) of 60–120 s. For optogenetic studies, light stimulation occurred only during the 30-s tones of this session. Following delivery of the last foot shock, mice remained in the conditioning chamber for a 2-min consolidation period. 24 h later, mice were placed into a separate conditioning box (Med Associates) that contained a white Plexiglas floor, a striped pattern on the walls, and was cleaned and scented with a 70% ethanol solution. After a 3 min baseline period, mice were presented with 10 tones (30 s, 3 kHz, 80 dB) with a 5 s ITI. Mice remained in the chamber after the last tone for a two-minute consolidation period. 24 h later (48 h after training), mice were returned to the original training chamber for 5 min. For each session, freezing behaviour was hand-scored every 5 s by a trained observer blinded to experimental treatment as described previously[24]. Freezing was defined as a lack of movement except as required for respiration.

Immunohistochemistry and histology. All mice used for behavioural and anatomical tracing experiments were anesthetized with Avertin and transcardially perfused with 30 ml of ice-cold 0.01 M PBS followed by 30 ml of ice-cold 4% paraformaldehyde (PFA) in PBS. Brains were extracted and stored in 4% PFA for 24 h at 4 °C before being rinsed twice with PBS and stored in 30% sucrose and PBS until the brains sank. 45 μm slices were obtained on a Leica VT100S and stored in 50/50 PBS/Glycerol at −20 °C. DREADD or ChR2-containing sections were mounted on slides, allowed to dry, coverslipped with VectaShield (Vector Labs, Burlingame, CA), and stored in the dark at 4 °C.

Tryptophan hydroxylase/Fluoro-Gold/c-fos triple labelling. We stained free-floating dorsal raphe sections using indirect immunofluorescence sequentially for first tryptophan hydroxylase (TPH) and Fluoro-Gold (FG) and then c-*fos*. For TPH/FG, we washed sections 3× for 5 min with 0.01 M PBS, permeabilized them for 30 min in 0.5% Triton/0.01 M PBS, and washed the sections again 2× with 0.01 M PBS. We blocked the sections for 1 h in 0.1% Triton/0.01 M PBS containing 10% (v/v) normal donkey serum and 1% (w/v) bovine serum albumin (BSA). We then added primary antibodies (1:500 mouse anti-TPH (Sigma Aldrich T0678) and 1:3,000 guinea-pig anti-Fluoro-Gold (Protos Biotech NM101)) to blocking buffer and incubated the sections overnight at 4 °C. The next day, we washed the sections 3× for 5 min with 0.01 M PBS, then incubated them with 1:500 with Alexa Fluor 647-conjugated donkey anti-mouse and Alexa Fluor 488-conjugated donkey anti-guinea pig secondary antibodies for 2 h at room temperature, and washed the sections 4× for 5 min with 0.01 M PBS. We then proceeded directly to the c-*fos* tyramide signal amplification based immunofluorescent staining. We permeabilized

the sections in 50% methanol for 30 min, then quenched endogenous peroxidase activity in 3% hydrogen peroxide for 5 min. Followed by two 10 min washes in 0.01 M PBS, we blocked the sections in PBS containing 0.3% Triton X-100 and 1.0% BSA for 1 h. c-fos primary antibody (Santa Cruz Biotechnology, -sc-52) was added to sections at 1:3,000 and sections were incubated for 48 h at 4 °C. On day 3, we washed the sections in TNT buffer (0.1 M Tris-HCl pH 7.5, 0.15 M NaCl, 0.05% Tween-20) for 10 min, blocked in TNB buffer (0.1 M Tris-HCl pH 7.5, 0.15 M NaCl, 0.5% blocking reagent – PerkinElmer FP1020) buffer for 30 min. We then incubated the sections in secondary antibody (goat anti-rabbit HRP-conjugated PerkinElmer) 1:200 in TNB buffer for 30 min, washed the sections in TNT buffer 4× for 5 min, and then incubated the sections in Cy3 dye diluted in TSA amplification diluents for 10 min. We washed the sections 2× in TNT buffer, mounted them on microscope slides. We coverslipped the slides using Vectashield mounting medium. We acquired 4–5 of 2 × 4 tiled *z*-stack (5 optical slices comprising 7 μm total) images of the dorsal raphe from each naive and shock mouse on a Zeiss 800 upright confocal microscope. Scanning parameters and laser power were matched between groups. Images were preprocessed using stitching and maximum intensity projection and then analysed using an advanced processing module in Zeiss Zen Blue that allows nested analysis of multiple segmented fluorescent channels within parent classes. Double-labelled and triple-labelled cells were validated in a semi-automated fashion. At least 4 sections per mouse were counted in this way. One mouse was identified as a significant outlier in the shock group and was excluded from further analysis.

***Sert*^{Cre}::ChR2, *and Crf*$^{Intrsect\text{-}ChR2}$ validation.** To verify expression of ChR2-expressing fibres in the BNST originating from DRN serotonergic neurons, 300 μm slices used for *ex vivo* electrophysiological recordings containing the DRN and BNST were stored in 4% paraformaldehyde at 4 °C for 24 h before being rinsed with PBS, mounted, and coverslipped with Vectashield mounting medium. Images showing eYFP fluorescence from the DRN and BNST were obtained on a Zeiss 800 upright confocal microscope using a 10× objective and tiled *z* stacks. To validate the INTRSECT construct, mice received injections of HSV-hEF1α-mCherry or HSV-ef1α-LSL1-mCherry-IRES-flpo to both the LH and VTA bilaterally ($n = 4$ and 5, respectively). Both groups received AAVDJ-hSyn-Cre-on/Flp-off-hChR2(H134R)-EYFP to the BNST bilaterally. Six weeks following injection, mice were perfused and tissue was collected as described above. To visualize YFP expression in the BNST of *Crf*^{Cre}::Intrsect^{BNST} mice, free-floating slices containing the BNST were rinsed three times with PBS for 5 min each. Slices were then incubated in 50% methanol for 30 min then incubated in 3% hydrogen peroxide for 5 min. Following three 10-min washes in PBS, slices were incubated in 0.5% Triton X-100 for 30 min followed by a 10 min PBS wash. Slices were blocked in 10% normal donkey serum/0.1% Triton X-100 for 1 h, and then they were incubated overnight at 4°C with a primary chicken anti-GFP antibody (GFP-1020, Aves) at 1:500 in blocking solution. Following primary incubation, slices were rinsed three times with 0.01M PBS for 10 min each and incubated with a fluorescent secondary antibody (AlexaFluor 488 donkey anti-chicken) at 1:200 in PBS for 2 h at room temperature. Slices were then rinsed with four 10-min PBS washes before being mounted onto glass slides and coverslipped with Vectashield with DAPI. A 3 × 4 tiled *z* stack (7 optical sections comprising 35 μm total) image from both the left and right hemispheres of the BNST was obtained at 20× magnification using a Zeiss 800 upright confocal microscope. Scanning parameters and laser power were matched between groups. Images were preprocessed using stitching and maximum-intensity projection. The number of fluorescent cells in the dorsal and ventral aspects of the BNST were counted by a blinded scorer using the cell counter plug-in in FIJI (ImageJ). Each hemisphere was considered independently per mouse. One mouse in the flp-expressing group was a significant outlier for number of cells expressed in a ventral BNST hemisphere (ROUT, Q = 0.1%) and all data from that mouse were excluded.

Choleratoxin retrograde tracer studies in CRF reporter mice. 3 male CRF-L10a reporter mice were injected with 200 nl of CTB 555 and CTB 647 bilaterally to the LH and VTA, respectively, as described above. 5 days following injection, mice were perfused as described above, the brains were extracted, and were stored in 4% paraformaldehyde for 24 h at 4 °C before being rinsed with PBS and transferred to 30% sucrose until the brains sank. 45 μm sections containing the BNST were collected as described above. Sections containing the BNST were mounted on glass slides and coverslipped using Vectashield. An image from the left and right hemispheres of a medial section of the BNST was obtained on a Zeiss 800 upright microscope using a 20×objective and 3 × 5 tiled *z* stacks (5 optical slices comprising 7 μm total). Images were preprocessed using stitching and maximum intensity projection, and were then analysed using the cell counter function in FIJI (ImageJ). Only cells positive for GFP (putative CRF neurons) were considered. Cells were scored exclusively as either 555+ only (LH-projecting), 647+ only (VTA-projecting), 555+ and 647+ (projecting to both LH and VTA), or 555− and 647− (unlabelled; neither LH- nor VTA- projecting). The total number of CRF neurons scored was calculated as the sum of all four groups, and percentages of each type were calculated from this value. Each hemisphere was scored and plotted independently ($n = 6$ images from 3 mice), and the dorsal and ventral BNST were considered separately. The average values were plotted as pie charts (Extended Data Fig. 5).

Double fluorescence *in situ* hybridization (FISH). For validation of 2C-cre line and comparison of CRF/2C mRNA cellular co-localization, mice were anesthetized using isoflurane, rapidly decapitated, and brains rapidly extracted. Immediately after removal, the brains were placed on a square of aluminium foil on dry ice to freeze. Brains were then placed in a −80°C freezer for no more than 1 week before slicing. 12 μm slices were made of the BNST on a Leica CM3050S cryostat (Germany) and placed directly on coverslips. FISH was performed using the Affymetrix ViewRNA 2-Plex Tissue Assay Kit with custom probes for CRF, 5-HT_{2C}, and Cre designed by Affymetrix (Santa Clara, CA). Slides were coverslipped with SouthernBiotech DAPI Fluoromount-G. (Birmingham, AL). 3 × 5 tiled *z* stack (15 optical sections comprising 14 μm total) images of the entire 12 μm slice were obtained on a Zeiss 780 confocal microscope for assessment of CRF/2C colocalization. A single-plane 40× tiled image of a CRF/2C slice was obtained on a Zeiss 800 upright confocal microscope for the magnified image shown in Extended Data 6b, right. 3 × 5 tiled *z* stack (7 optical sections comprising 18 μm) images of 2C/Cre slices were obtained on a Zeiss 800 upright confocal microscope for the 2C/Cre validation. All images were preprocessed with stitching and maximum intensity projection. An image of the BNST from 3 mice in each condition was hand counted for each study using the cell counter plugin in FIJI (ImageJ). Cells were classified into three groups: probe 1^+, probe 2^+, or probe 1 and 2^+. Only cells positive for a probe were considered. Results are plotted as average classified percentages across the three images.

Group assignment. No specific method of randomization was used to assign groups. Animals were assigned to experimental groups so as to minimize the influence of other variables such as age or sex on the outcome.

Inclusion/exclusion criteria. Pre-established criteria for excluding mice from behavioural analysis included (1) missed injections, (2) anomalies during behavioural testing, such as mice falling off the elevated plus maze, (3) damage to or loss of optical fibres, (4) statistical outliers, as determined by the Grubb's test.

Sample size. A power analysis was used to determine the ideal sample size for behaviour experiments. Assuming a normal distribution, a 20% change in mean and 15% variation, we determined that we would need 8 mice per group. In some cases, mice were excluded due to missed injections or lost optical fibres resulting in fewer than 8 mice per group. For electrophysiology experiments, we aimed for 5–7 cells from 3–4 mice.

Statistics. Data are presented as means ± s.e.m. For comparisons with only two groups, *P* values were calculated using paired or unpaired *t*-tests as described in the figure legends. Comparisons across more than two groups were made using a one-way ANOVA, and a two-way ANOVA was used when there was more than one independent variable. A Bonferroni post-test was used following significance with an ANOVA. In cases in which ANOVA was used, the data met the assumptions of equality of variance and independence of cases. If the condition of equal variances was not met, Welch's correction was used. Some of the sample groups were too small to detect normality (<8 samples) but parametric tests were used because nonparametric tests lack sufficient power to detect differences in small samples (Graphpad Statistics Guide – http://www.graphpad.com). The standard error of the mean is indicated by error bars for each group of data. Differences were considered significant at *P* values below 0.05. All data were analysed with GraphPad Prism software.

21. Krashes, M. J. *et al.* An excitatory paraventricular nucleus to AgRP neuron circuit that drives hunger. *Nature* **507,** 238–242 (2014).
22. Madisen, L. *et al.* A robust and high-throughput Cre reporting and characterization system for the whole mouse brain. *Nature Neurosci.* **13,** 133–140 (2010).
23. Bath, B. D. *et al.* Subsecond adsorption and desorption of dopamine at carbon-fiber microelectrodes. *Anal. Chem.* **72,** 5994–6002 (2000).
24. Hefner, K. *et al.* Impaired fear extinction learning and cortico-amygdala circuit abnormalities in a common genetic mouse strain. *J. Neurosci.* **28,** 8074–8085 (2008).

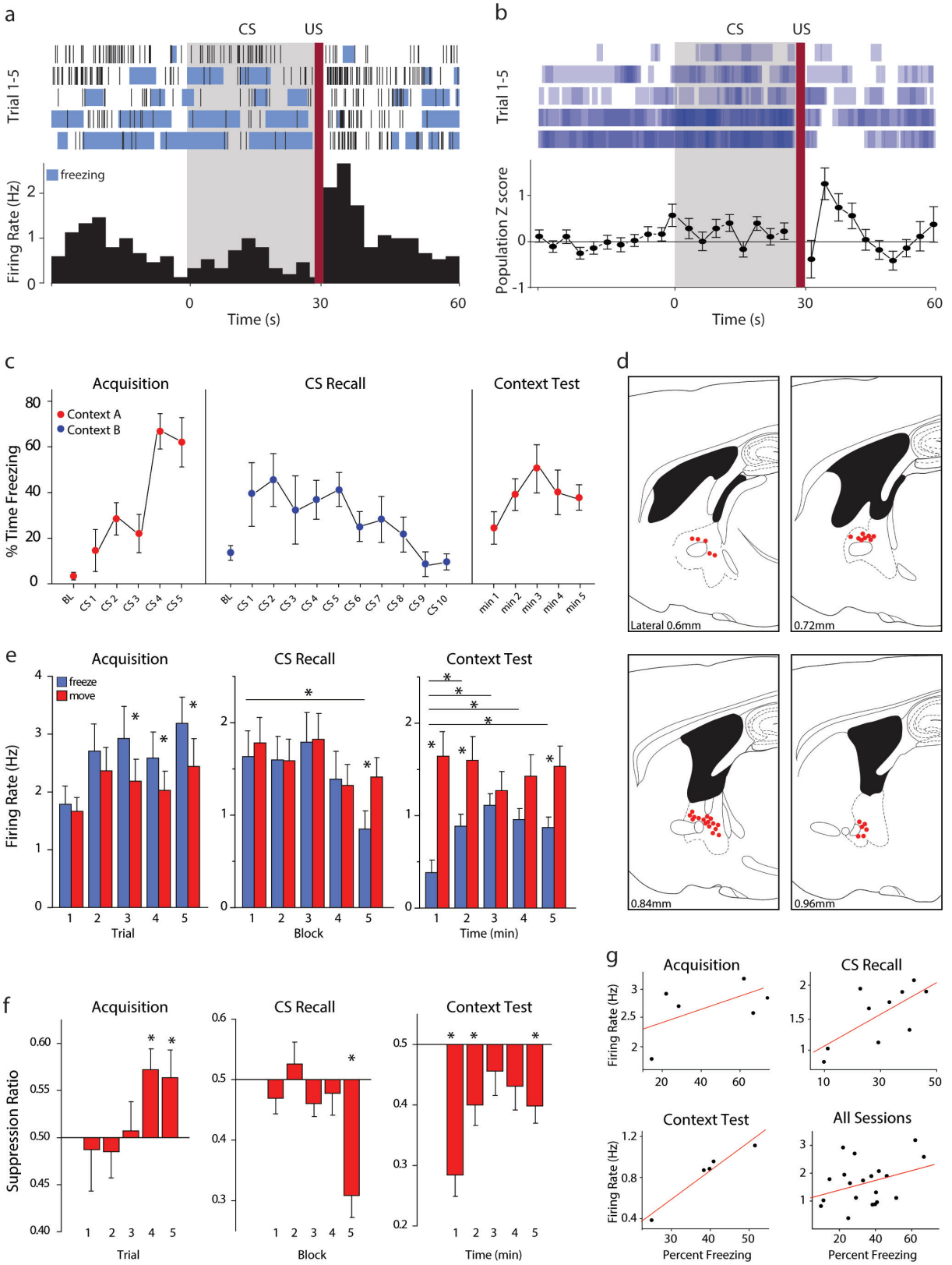

Extended Data Figure 1 | See next page for caption.

Extended Data Figure 1 | *In vivo* recordings in BNST neurons during fear conditioning reveal opposite patterns of activation during acquisition and recall. a, **b**, Representative neuronal firing rate (**a**) and population *Z* score of the firing rate (**b**) for BNST neurons ($n = 45$ cells from 7 mice) 30 s before conditioned stimulus (tone), during the conditioned stimulus (CS), and 30 s after the unconditioned stimulus. **c**, Percentage time spent freezing during fear acquisition, cued fear recall and contextual fear recall. **d**, Electrode placements for BNST recordings. **e**, Raw firing rates during freezing (blue) versus movement (red) epochs were averaged across all putative principal neurons (firing rate < 10 Hz). Acquisition: cells in BNST exhibited greater average firing rates during freezing epochs compared to movement epochs during CS3 ($t_{44} = 2.88$, $P < 0.01$, Student's unpaired two-tailed *t*-test), CS4 ($t_{44} = 3.14$, $P < 0.01$, Student's unpaired two-tailed *t*-test), and CS5 ($t_{44} = 4.4$, $P < 0.001$, Student's unpaired two-tailed *t*-test) ($n = 45$ cells from 7 mice). CS recall: average firing rates during freezing epochs decreased over CS presentations such that firing during block 5 was significantly less than block 1 ($t_{41} = 3.44$, $P = 0.001$, Student's unpaired two-tailed *t*-test). Freezing firing rates during block 5 were also significantly less than movement epochs during block 5 ($t_{41} = 4.03$, $P < 0.001$, Student's unpaired two-tailed *t*-test) ($n = 42$ cells from 7 mice). CX test: average firing rate was significantly greater during movement versus freezing epochs during minute 1 ($t_{44} = 4.83$, $P < 0.001$, Student's unpaired two-tailed *t*-test), minute 2 ($t_{44} = 3.17$, $P < 0.01$, Student's unpaired two-tailed *t*-test), and minute 5 ($t_{44} = 4.36$, $P < 0.001$, Student's unpaired two-tailed *t*-test) ($n = 45$ cells from 7 mice). **f**, Freezing-related changes in firing rates during the CS were determined by measuring the ratio of average firing rates during freezing versus movement epochs for each session. Acquisition: activity during freezing epochs increased significantly relative to movement epochs during CS4 ($t_{45} = 3.26$, $P < 0.01$, Student's unpaired two-tailed *t*-test) and CS5 ($t_{45} = 2.17$, $P < 0.05$, Student's unpaired two-tailed *t*-test) ($n = 46$ cells from 7 mice). CS recall: freezing significantly suppressed activity relative to movement epochs during the last two CS presentations ($t_{47} = 5.29$, $P = <0.001$, Student's unpaired two-tailed *t*-test) ($n = 48$ cells from 7 mice). CX test: freezing significantly suppressed activity during minutes 1 ($t_{44} = 6.06$, $P < 0.001$, Student's unpaired two-tailed *t*-test), minute 2 ($t_{44} = 2.92$, $P < 0.01$, Student's unpaired two-tailed *t*-test), and minute 5 ($t_{44} = 3.55$, $P = .001$, Student's unpaired two-tailed *t*-test) ($n = 45$ cells from 7 mice). **g**, Plots showing correlation between freezing behaviour and firing rate of BNST neurons across sessions and for all sessions. Data are mean ± s.e.m. $^{*}P < 0.05$ $^{**}P < 0.01$; $^{***}P < 0.001$. Scale bar, 100 μm.

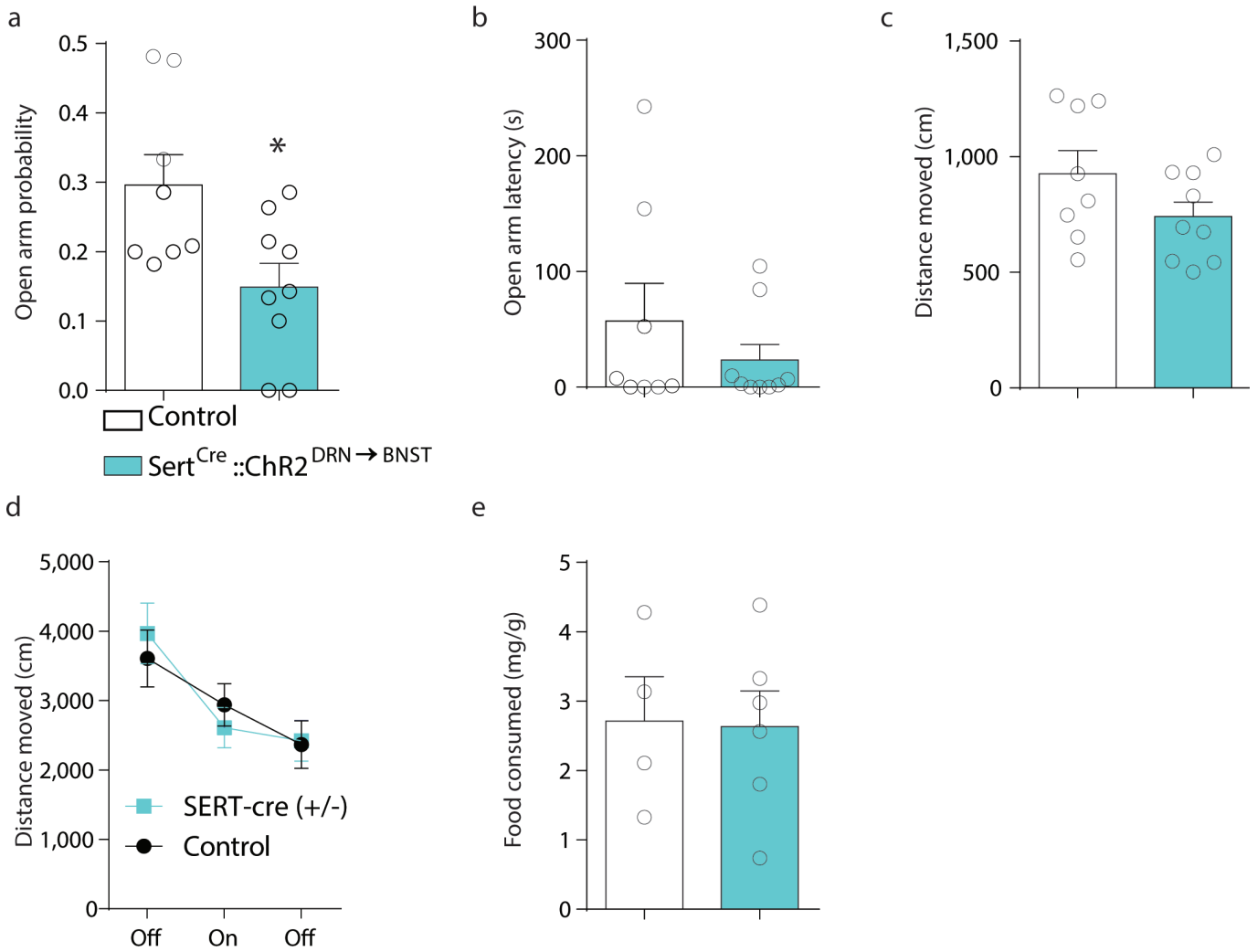

Extended Data Figure 2 | Effects of optogenetic stimulation of 5-HT inputs to the BNST on feeding, anxiety and locomotion. **a**–**c**, $Sert^{Cre}$::ChR2$^{DRN\rightarrow BNST}$ mice exhibited reduced probability ($t_{15} = 2.67$, $P < 0.05$, Student's unpaired two-tailed t-test, $n = 8$ control, $n = 9$ ChR2) and latency ($t_{15} = 1.003$, $P > 0.05$, Student's unpaired two-tailed t-test, $n = 8$ control, $n = 9$ ChR2) to enter the open arms of the EPM without exhibiting locomotor deficits. **d**, **e**, Photostimulation of 5-HT$^{DRN\rightarrow BNST}$ terminals had no effect on locomotor activity in the open field (**d**) ($n = 9$ control, $n = 11$ ChR2) or home cage feeding (**e**) ($n = 4$ control, $n = 6$ ChR2). Data are mean ± s.e.m. *$P < 0.05$.

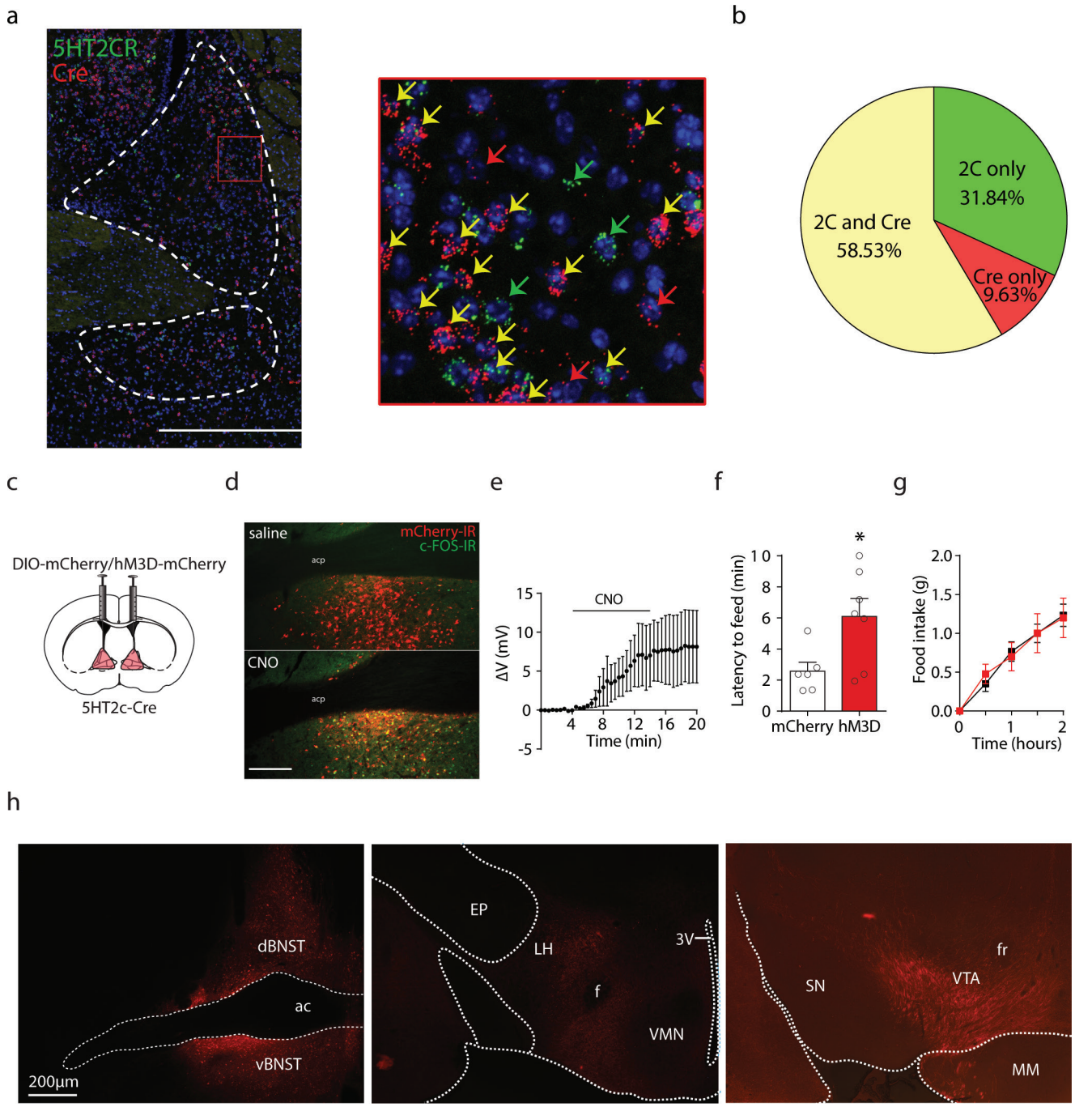

Extended Data Figure 3 | Chemogenetic activation of 5-HT$_{2C}$R-expressing neurons in the BNST increases anxiety-like behaviour. **a**, Confocal images of coronal BNST slices obtained from *Htr2c*^{Cre} mice following double fluorescence *in situ* hybridization for 5-HT$_{2C}$R and Cre. Yellow arrows indicate cells in which there is co-localization, red arrows indicate cells in which only Cre is expressed and green arrows indicate cells in which only 5-HT$_{2C}$R is expressed. **b**, Pie chart representing the distribution of genetic markers in BNST neurons. **c**, Experimental configuration in *Htr2c*^{cre}::hM3Dq^{BNST} mice. **d**, Coronal images showing c-fos induction in 5-HT$_{2C}$R expressing neurons in the BNST of *Htr2c*^{Cre}::hM3Dq^{BNST} or *Htr2c*^{Cre}::mCherry^{BNST} mice following CNO injection. **e**, Bath application of CNO depolarized 5-HT$_{2C}$R-expressing neurons expressing hM3Dq in slice ($n = 3$ cells from 3 mice). **f**, Chemogenetic stimulation of 5-HT$_{2C}$R expressing neurons in BNST increased latency to feed in the NSF ($t_{11} = 2.591$, $P < 0.05$, Student's unpaired two-tailed t-test, $n = 6$; mCherry, $n = 7$ hM3Dq). **g**, Chemogenetic activation of 5-HT$_{2C}$R-expressing BNST neurons had no effect on home cage feeding ($n = 5$ mCherry, $n = 6$ hM3Dq). **h**, Confocal images from *Htr2c*^{Cre}::mCherry^{BNST} mice showing mCherry expression in 5-HT$_{2C}$R-expressing soma in the BNST and fibres in the LH and VTA. Data are mean ± s.e.m. *$P < 0.05$. Scale bar, 100 µm.

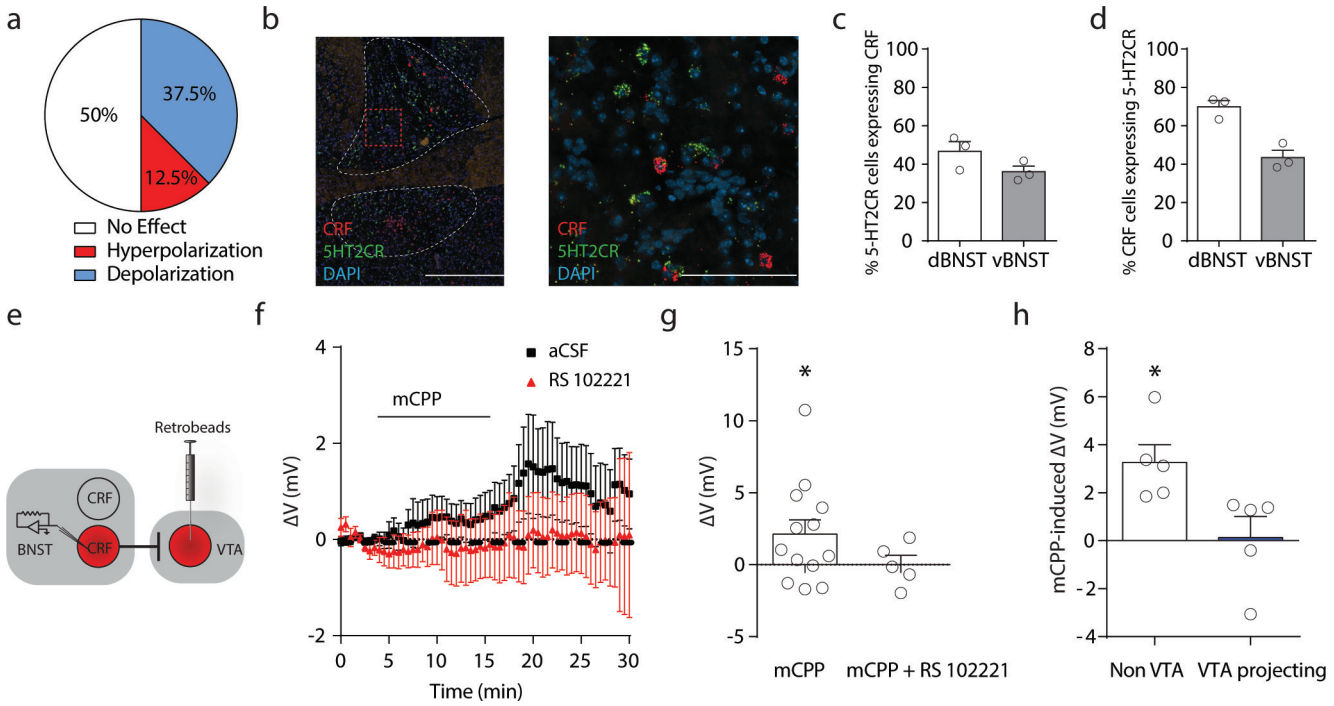

Extended Data Figure 4 | Electrophysiological characterization of 5-HT responses and 5-HT receptor expression in CRF^{BNST} neurons. **a**, A pie chart showing the distribution of CRF^{BNST} neurons that were depolarized, hyperpolarized, or had no response to 5-HT ($n = 8$ cells from 4 mice). **b**, Coronal images of the BNST showing co-localization of 5-HT_{2C}Rs with CRF mRNA using double fluorescence *in situ* hybridization. **c**, **d**, Histograms showing the percentage of 5-HT_{2C} neurons that express CRF and the percentage of CRF neurons that express 5-HT_{2C}Rs in the BNST ($n = 3$ slices from 3 mice). **e**, Recording configuration in CRF^{BNST} neurons. **f**, Slice electrophysiology in BNST of *Crf* reporter mice showing depolarization of all (VTA-projecting and non-projecting) CRF neurons following bath application of the 5-HT_2 receptor agonist mCPP ($n = 12$ cells from 6 mice) and blockade of this response by the 5-HT_{2C} receptor antagonist RS-102221 ($n = 5$ cells from 3 mice). **g**, Change in membrane potential induced by mCPP ($t_{12} = 2.18$, $P < 0.05$, one-sample *t*-test, $n = 13$ cells from 6 mice) is blocked by a 5-HT_{2C}R antagonist ($n = 5$ cells from 3 mice). **h**, mCPP selectively depolarizes non-VTA-projecting CRF^{BNST} neurons ($n = 5$ cells from 2 mice non-VTA-projecting CRF, $n = 5$ cells from 4 mice VTA-projecting CRF). Data are mean ± s.e.m. $^*P < 0.05$.

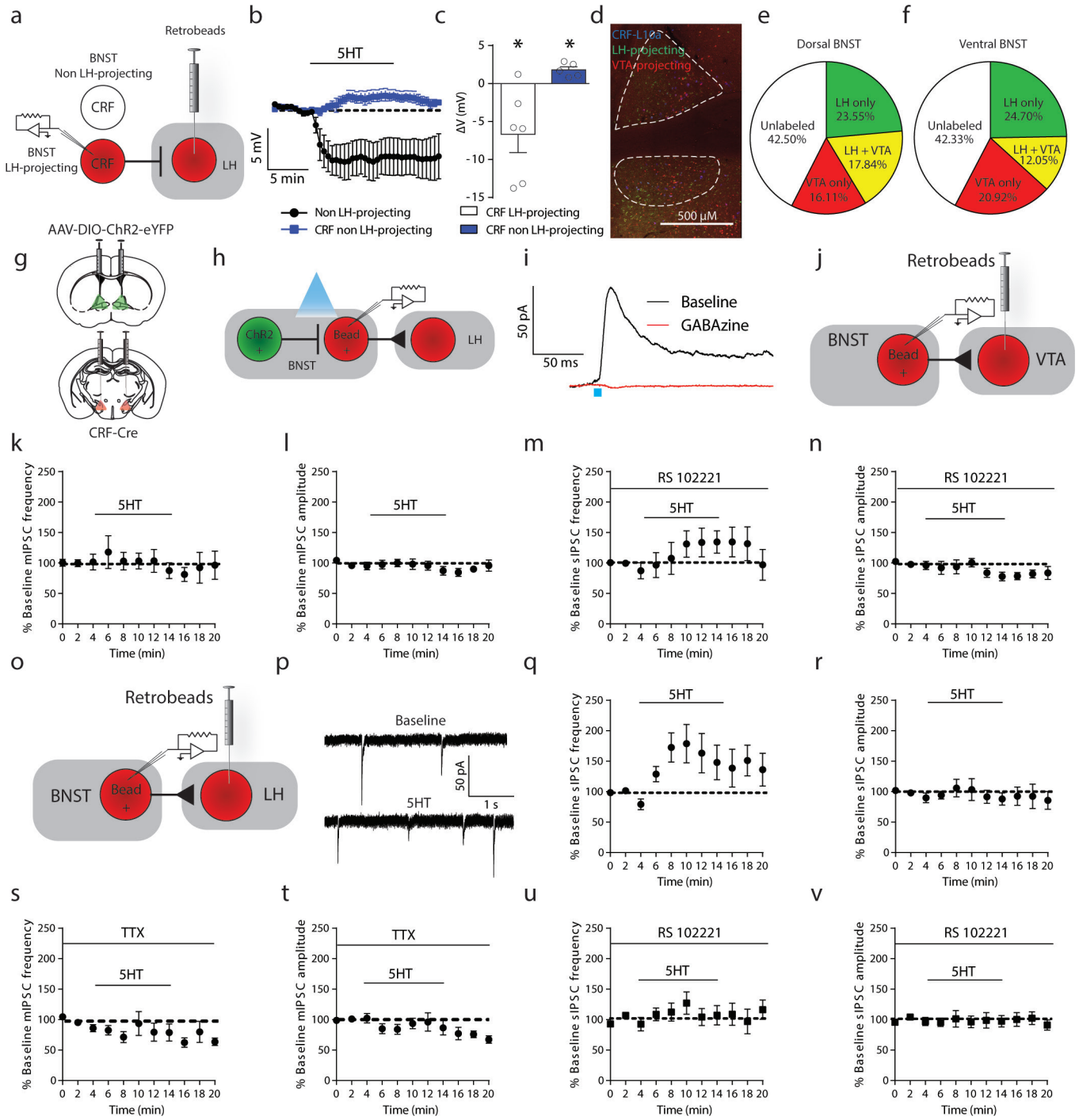

Extended Data Figure 5 | 5-HT activates inhibitory microcircuits in the BNST that modulate outputs to the LH. a, Recording configuration in CRF reporter mice infused with retrograde tracer beads in the LH. **b**, Average traces of 5-HT induced depolarization in LH projecting versus non-projecting neurons. **c**, Histograms showing 5-HT induced depolarization in non-LH projecting BNST neurons ($t_4 = 4.425$, $P < 0.05$, one-sample t-test, $n = 5$ cells from 3 mice) and hyperpolarization in LH-projecting neurons ($t_5 = 2.789$, $P < 0.05$, one-sample t-test, $n = 6$ cells from 3 mice). **d**, Confocal image of retrogradely CTB-labelled VTA (red) and LH (green) outputs in a *CRF-L10a* reporter (blue). **e**, **f**, Pie charts depicting the percentage of LH-projecting only, VTA-projecting only, collateralizing, and CTB-negative (unlabelled) CRF in neurons in the dorsal and ventral aspects of the BNST ($n = 6$ hemispheres from 3 mice). **g**, Experimental schematic depicting viral infusions into the BNST and retrograde tracer bead infusions into the LH of Crf^{Cre}::ChR2^{BNST} mice. **h**, Recording configuration in Crf^{Cre}::ChR2^{BNST} mice with LH tracer beads. **i**, Representative trace of light evoked IPSCs in LH-projecting neurons ($n = 7$ cells from 4 mice) and blockade of this light evoked response by GABAzine ($n = 2$ cells from 2 mice). **j**, Recording configuration in VTA-projecting neurons in the BNST of C57BL/6 mice. **k**, **l**, 5-HT has no effect on miniature IPSC frequency or amplitude in BNST→VTA projecting neurons ($n = 7$ from 4 mice). **m**, **n**, 5-HT has no effect on sIPSC frequency or amplitude in the presence of the 5-HT$_{2C}$R antagonist RS-102221 ($n = 5$ cells from 4 mice). **o**, Recording configuration in LH projecting neurons in the BNST of C57BL/6 mice. **p**, Representative traces showing an increase in sIPSC frequency in the presence of 5-HT for 6 cells from 3 mice. **q**, **r**, 5-HT increases sIPSC frequency but not amplitude in BNST→LH projecting neurons ($F_{11,55} = 11.65$, $P < 0.01$, repeated measures one-way ANOVA, $n = 6$ cells from 3 mice). **s**, **t**, 5-HT has no effect on miniature IPSC frequency or amplitude ($n = 5$ cells from 3 mice). **u**, **v**, 5-HT has no effect on sIPSC frequency or amplitude in the presence of RS-102221 ($n = 6$ cells from 4 mice). Data are mean ± s.e.m. $^*P < 0.05$.

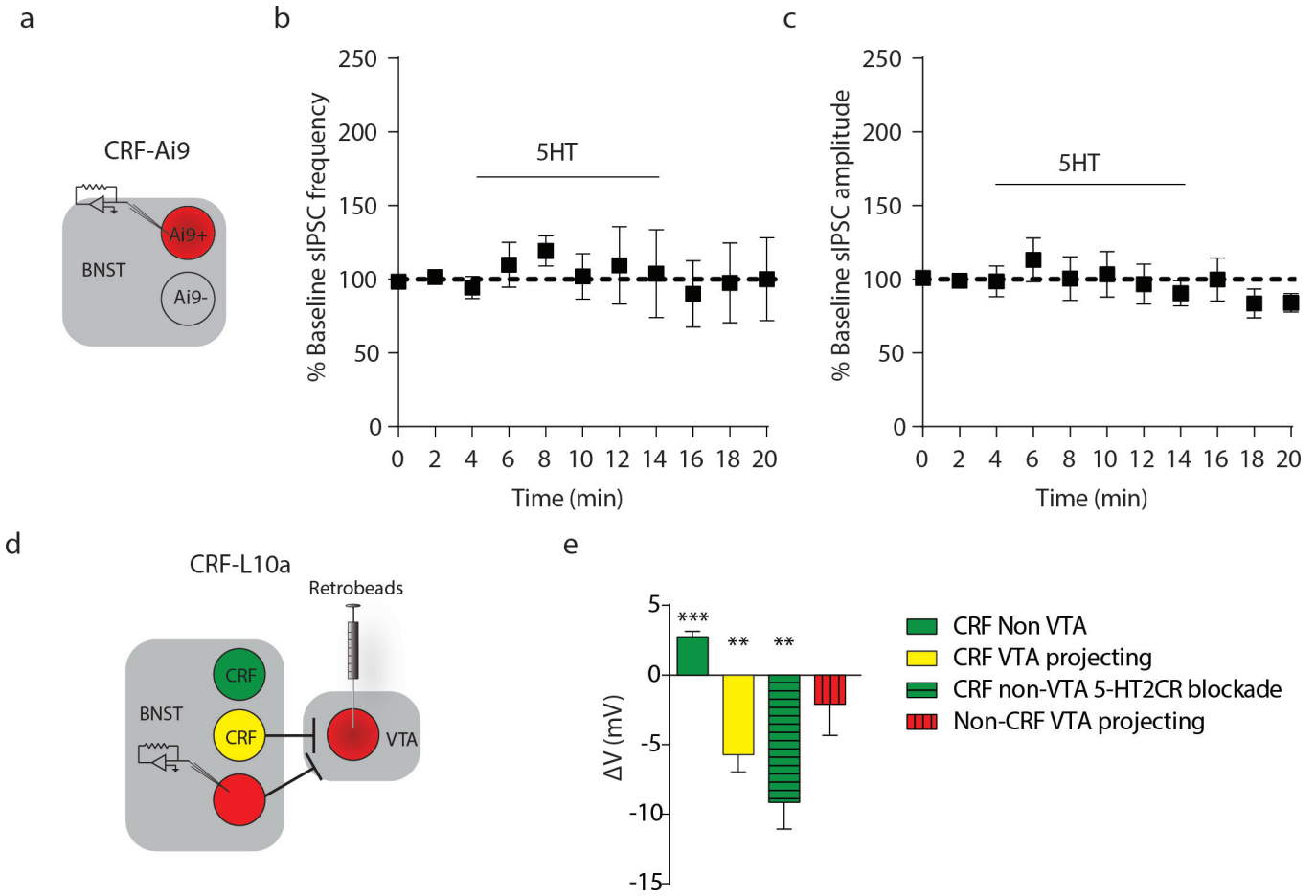

Extended Data Figure 6 | 5-HT does not alter GABAergic transmission in CRF neurons nor does it directly excite non-CRF VTA-projecting neurons in the BNST. a, Recording configuration in CRF^{BNST} neurons in a CRF reporter. **b**, **c**, 5-HT has no effect on sIPSC frequency or amplitude in the total population of CRF neurons ($n = 5$ cells from 3 mice). **d**, Recording configuration in non-CRF, VTA-projecting neurons in the BNST and average trace of 5-HT effect on membrane potential in non-CRF, VTA-projecting neurons in the presence of tetrodotoxin. **e**, Histogram summarizing 5-HT effects on membrane potential in local and VTA-projecting CRF neurons and local CRF neurons in the presence of the $5\text{-}HT_{2C}$ receptor antagonist RS-102221 (same data shown in Fig. 2b) juxtaposed with the lack of effect of 5-HT on membrane potential in non-CRF, VTA-projecting neurons ($t_4 = 0.9381$, ns, one-sample t-test, $n = 5$ cells from 3 mice). Data are mean ± s.e.m. $^{**}P < 0.01$; $^{***}P < 0.001$.

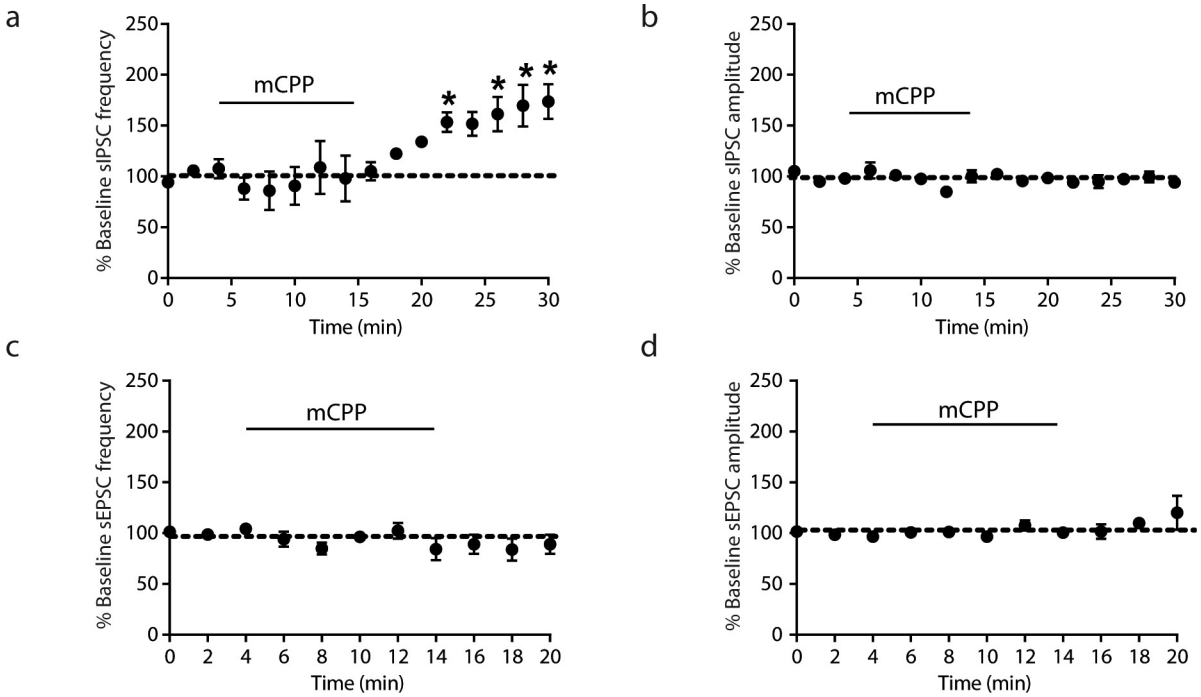

Extended Data Figure 7 | The 5-HT$_2$ agonist mCPP increases GABAergic but not glutamatergic transmission in the BNST. **a**, **b**, mCPP increases sIPSC frequency ($F_{15,30} = 1.863$, $P < 0.001$, Repeated measures one-way ANOVA, $n = 3$ cells from 3 mice) but not amplitude in the BNST of C57BL/6 mice. **c**, **d**, mCPP has no effect on spontaneous excitatory postsynaptic current (sEPSC) frequency or amplitude in the BNST of C57BL/6 mice ($n = 5$ cells from 3 mice). Data are mean ± s.e.m. *$P < 0.05$.

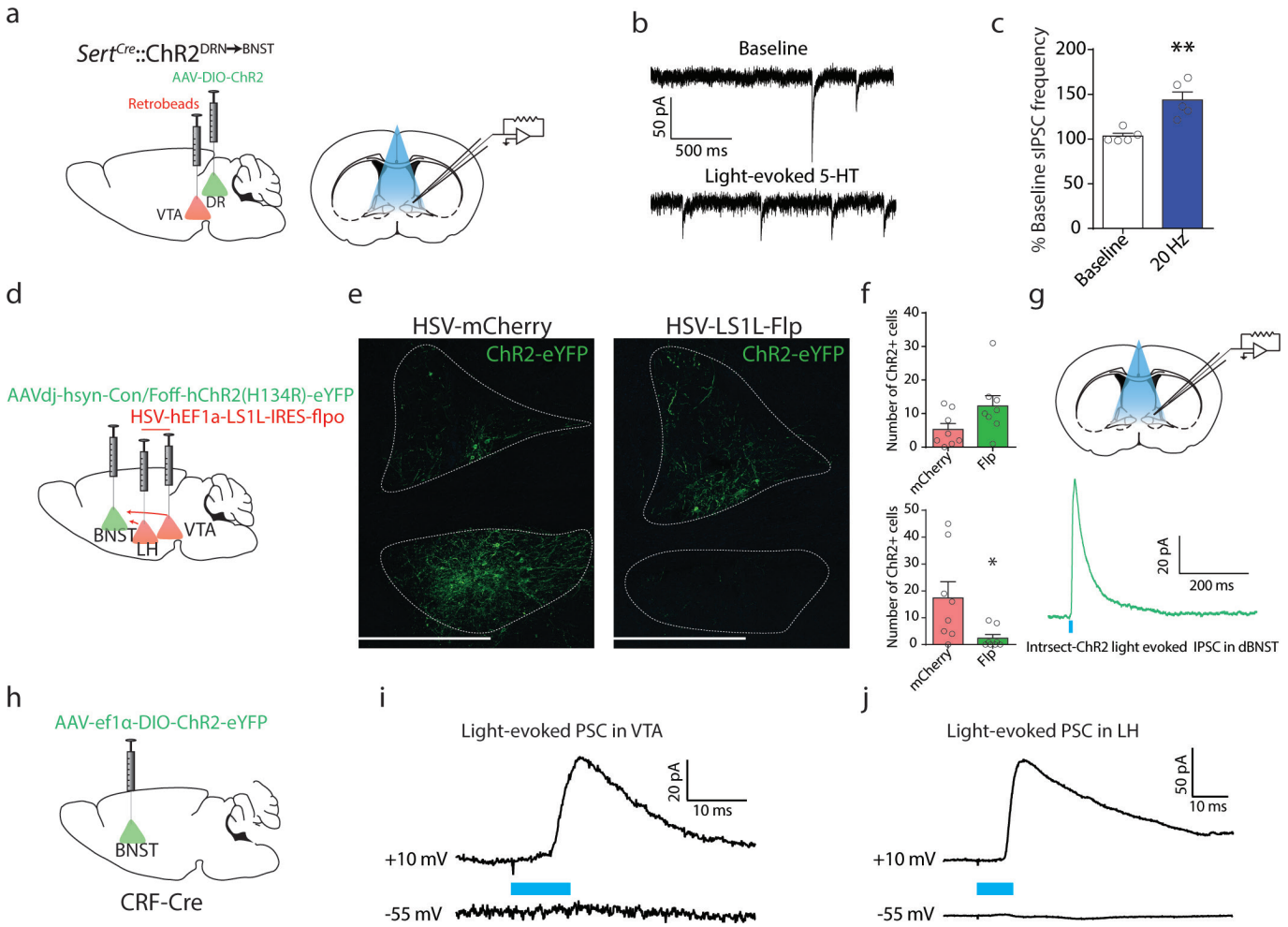

Extended Data Figure 8 | Optogenetic and intrsectional characterization of 5-HT-CRF circuits in the BNST and outputs to the midbrain. **a**, Experimental design and recording configuration from $Sert^{Cre}$::ChR2$^{DRN\rightarrow BNST}$ mouse with retrograde tracer beads in the VTA. **b**, Representative traces for 5 cells from 3 mice depicting the increase in sIPSCs in VTA-projecting neurons in the BNST following light-evoked 5-HT release. **c**, Histogram summarizing the effect of light evoked 5-HT release on sIPSC frequency in VTA-projecting neurons ($t_4 = 4.890$, $P < 0.01$, one-sample t-test, $n = 5$ cells from 3 mice). **d**, Experimental configuration in Crf^{Cre}::Intrsect-ChR2^{BNST} mice. **e**, Representative images from 4 Crf^{Cre}::HSV-LSL1-mCherry-flpo$^{VTA/LH}$ mice and 4 Crf^{Cre}::HSV-LSL1-mCherry$^{VTA/LH}$ mice injected with Intrsect-ChR2-eYFP in the BNST. **f**, Cell counts of eYFP$^+$ neurons from HSV-LSL1-flpo and HSV-LSL1-mCherry injected Crf^{Cre}::Intrsect-ChR2^{BNST} mice indicating the number of non-projecting CRF neurons compared to the total CRF population in the dorsal (top panel; $t_{14} = 1.959$, ns, Student's unpaired two-tailed t-test, $n = 4$ mice, 8 hemispheres per group) and ventral aspects of the BNST (bottom panel; $t_7 = 2.431$, $P < 0.05$, Student's unpaired Welch's corrected two-tailed t-test, $n = 4$ mice, 8 hemispheres per group). **g**, Recording configuration and light-evoked IPSC showing local GABA release from non-projecting CRF neurons in the BNST. **h**, Sterotaxic injection of ChR2 in Crf^{Cre} mouse. **i**, **j**, Light evoked IPSCs in the VTA and LH indicating that CRF projections to these regions are GABAergic. Data are mean ± s.e.m. $^*P < 0.05$; $^{**}P < 0.01$.

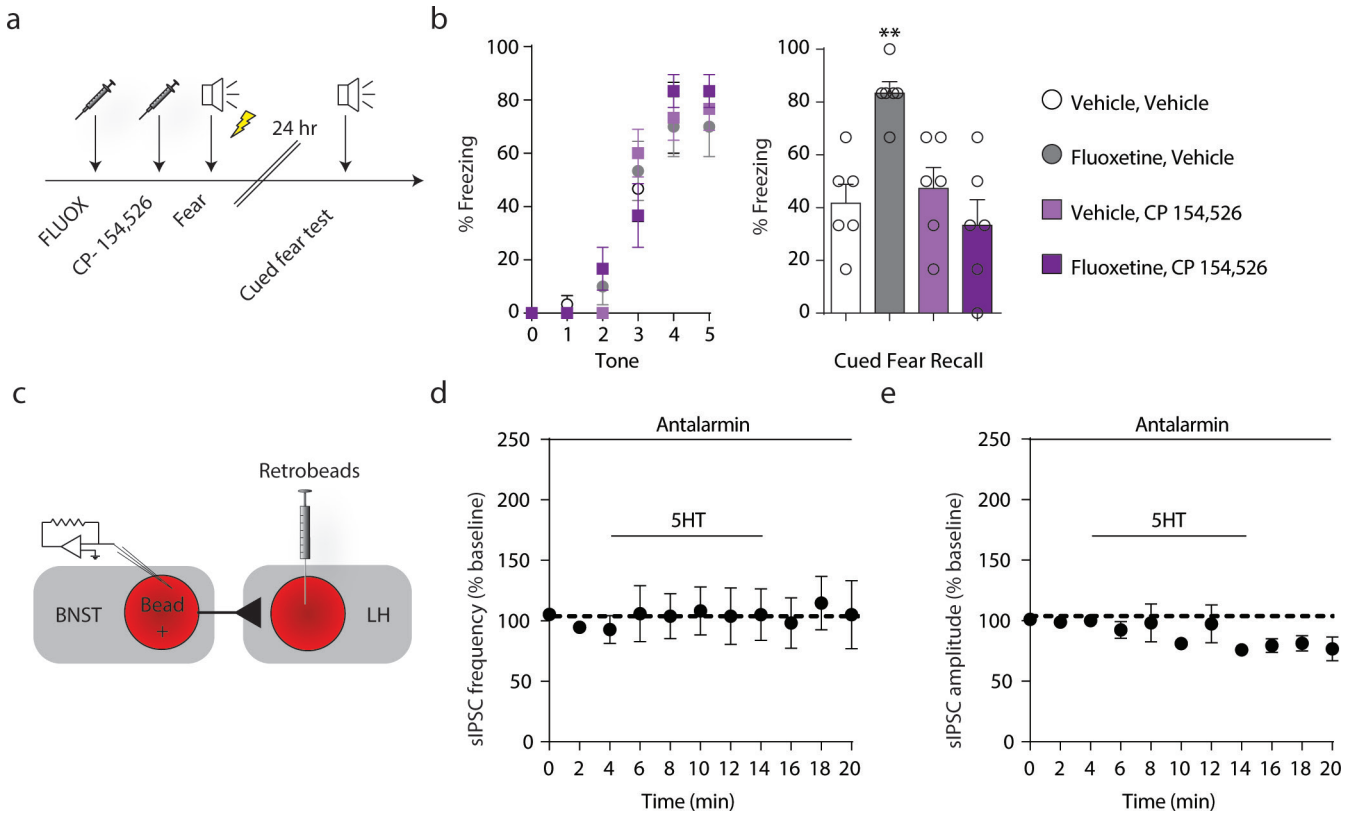

Extended Data Figure 9 | Pharmacological blockade of CRF_1 receptors reduces fluoxetine-induced aversive behaviour and 5-HT enhancement of GABAergic transmission in the BNST. a, Experimental schedule of injections and behaviour. **b**, CRF_1R antagonist does not modify fear acquisition but reduces fluoxetine enhancement of cued fear recall ($F_{1,20} = 13.70$, $P < 0.01$, two-way ANOVA, $n = 6$ per group). **c**, Recording configuration in BNST neurons that project to the LH in C57BL/6 mice. **d**, Bath application of a CRF_1R antagonist blocks the 5-HT induced increase in sIPSC frequency in LH-projecting neurons in the BNST ($F_{10,30} = 0.2213$, ns, Repeated measures one-way ANOVA, $n = 4$ cells from 2 mice). **e**, There was a reduction in sIPSC amplitude during 5-HT bath application and CRF_1R blockade ($F_{10,30} = 2.941$, $P < 0.05$, Repeated measures one-way ANOVA, $n = 4$ cells from 2 mice). Data are mean ± s.e.m. $^{**}P < 0.01$.

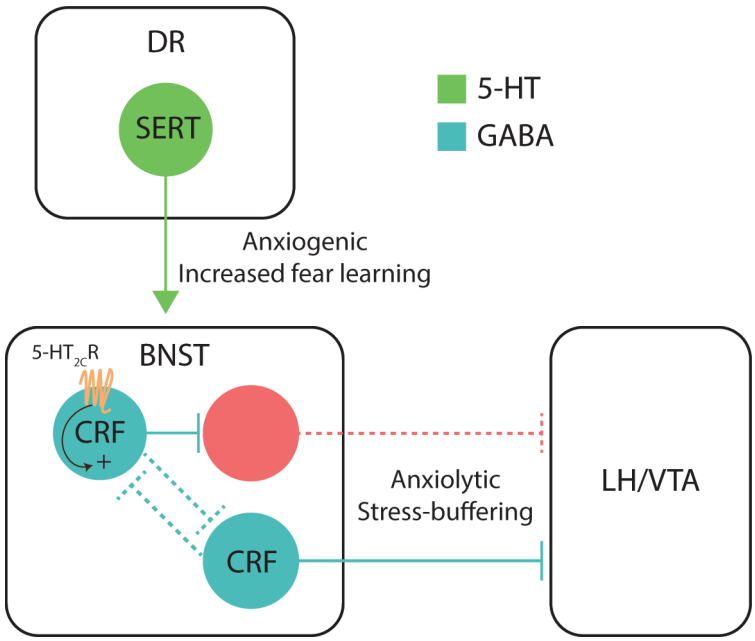

Extended Data Figure 10 | Model of a serotonin-sensitive inhibitory microcircuit in the BNST that modulates anxiety and aversive learning. Serotonin inputs to the BNST activate 5-HT_{2C}Rs expressed in non-projecting 'local' CRF neurons. These local CRF neurons promote anxiety and fear by inhibiting anxiolytic outputs to the VTA and LH that are putatively GABAergic. Another discrete subset of CRF neurons, which are inhibited by 5-HT, send direct, inhibitory projections to the VTA and LH. These CRF^{BNST} output neurons are GABAergic and putatively anxiolytic and stress buffering. Blue dashed lines indicate hypothesized additional synapses between CRF^{BNST} neurons. Dashed red line indicates a putatively GABAergic synapse.